

**ELASTO-PLASTIC FINITE ELEMENT ANALYSIS  
WITH SPECIAL REFERENCE TO REINFORCED CONCRETE**

by

**JOHN HON-SHING LAU**

**B.Sc., National Taiwan University, 1970**

**A THESIS SUBMITTED IN PARTIAL FULFILLMENT OF  
THE REQUIREMENTS FOR THE DEGREE OF  
MASTER OF APPLIED SCIENCE**

**in the Department**

**of**

**Civil Engineering**

**We accept this thesis as conforming to the  
required standard**

**THE UNIVERSITY OF BRITISH COLUMBIA**

**November, 1973**

In presenting this thesis in partial fulfilment of the requirements for an advanced degree at the University of British Columbia, I agree that the Library shall make it freely available for reference and study.

I further agree that permission for extensive copying of this thesis for scholarly purposes may be granted by the Head of my Department or by his representatives. It is understood that copying or publication of this thesis for financial gain shall not be allowed without my written permission.

Department of Civil Engineering

The University of British Columbia  
Vancouver 8, Canada

Date November 10, 1973

ABSTRACT

A numerical procedure is presented for the solution of elasto-plastic problems by means of the finite element approach. The incremental constitutive relationship from the Prandtl-Reuss equation is used in conjunction with the Von Mises yield criterion, the continuum being divided into triangular elements.

The Modified Newton-Raphson method is employed to solve the nonlinear incremental equilibrium equation. Numerical examples are studied and compared with the experimental and theoretical results in the literature.

The finite element program is also extended to nonlinear stress analysis of reinforced concrete structures.

TABLE OF CONTENTS

<u>Chapter</u>		<u>Page</u>
One	<u>Introduction</u>	1
Two	<u>Basic Definitions and Theories for Elasticity and Plasticity</u>	5
	I. Analysis of Stress	5
	II. Analysis of Strain	14
	III. Field Equations in Elasticity	18
	IV. Field Equations in Plasticity	20
Three	<u>Finite Element Method</u>	31
	I. Variational Principles	32
	II. Formulation of Finite Element Method by the Principle of Minimum Potential Energy	36
Four	<u>Formulation of Elasto-plastic Problems</u>	40
	I. General Considerations	40
	II. Generalized Incremental Equilibrium Equation	42
	III. Constitutive Equations: Elasto-Plastic Matrix	44
	IV. Solution of Plasticity Equations	51
	V. Procedures of Calculation	56
	VI. Examples	62
Five	<u>Nonlinear Stress Analysis of Reinforced Concrete</u>	78
	I. General Considerations	78
	II. Structural Idealization	79
	III. Failure Condition	80

<u>CHAPTER</u>		<u>Page</u>
Five	IV. <u>Calculation Procedure</u>	81
	V. Numerical Example	84
Six	<u>Conclusions</u>	98
Appendix		100
Bibliography		104

## TABLE OF FIGURES

## FIGURE

- 2-1 INTERNAL FORCES SYSTEM
- 2-2 STRESS VECTORS AND POSITIVE STRESS COMPONENTS
- 2-3 STRESS VECTORS ON A TETRAHEDRON
- 2-4 ROTATION OF COORDINATES
- 2-5 DISPLACEMENT OF NEIGHBORING POINTS
- 2-6 TRESCA YIELD SURFACE IN PRINCIPAL STRESS SPACE
- 2-7 VON MISES YIELD SURFACE IN PRINCIPAL STRESS SPACE
- 4-1 THE INCREMENTAL LOADING PROCESS
- 4-2 A COMBINATION OF THE LOAD INCREMENT AND  
NEWTON-RAPHSON (OR MODIFIED NEWTON-RAPHSON)  
METHOD
- 4-3 THE ILLUSTRATIONS OF EQS. (4-25), (4-26), (4-27),  
AND (4-28)
- 4-4a NEWTON-RAPHSON METHOD
- 4-4b MODIFIED NEWTON-RAPHSON METHOD
- 4-5 CONSTANT STRAIN ELEMENT
- 4-6 UNIFORMLY LOADED PERFORATED STRIP
- 4-7 UNIAXIAL STRESS-STRAIN CURVE
- 4-8 END LOAD vs. MAX STRAIN FOR PERFORATED STRIP
- 4-9a EXPERIMENTAL RESULTS
- 4-9b FINITE ELEMENT RESULTS

## FIGURE

- 4-10 EQUIVALENT STRESS vs. EQUIVALENT STRAIN IN  
THE ELEMENT WHICH YIELD FIRST
- 4-11 SHEAR WALL SUBJECTED TO LATERAL LOAD
- 4-12 UNIAXIAL STRESS-STRAIN CURVE
- 4-13 DEVELOPMENT OF PLASTIC ZONES FOR DIFFERENT  
VALUES OF
- 4-14a NORMAL STRESS DISTRIBUTION AT HIGHEST LOAD
- 4-14b SHEAR STRESS DISTRIBUTION AT HIGHEST LOAD
- 4-15a SHEAR STRESS DISTRIBUTION AT HIGHEST LOAD
- 4-16 RIGHT-ANGLE NOTCH: ELASTIC-PERFECTLY-PLASTIC
- 4-17 END LOAD vs. MAX. STRAIN FOR NOTCHED TENSION  
SPECIMEN. ELASTIC-PERFECTLY-PLASTICITY
- 4-18a D. ALLEN & R. SOUTHWELL'S SOLUTION
- 4-18b FINITE ELEMENT SOLUTION

LIST OF TABLES

TABLE 2-1	MAXIMUM SHEAR STRESS AND PRINCIPAL DIRECTION
TABLE 2-2	TRESCA YIELD CONDITION



### Acknowledgement

In 1972 the writer received from his supervisor, professor N.D. Nathan, two fundamental courses in solid mechanics, namely, Energy Theorems and The Finite element Method, which gave rise to the writer's interest in solid mechanics. The writer wishes to acknowledge the help that it has been: all of chapter three and most of chapter four and the appendix are based on a study of his lectures. The writer is also most grateful for his guidance, his reading and checking of the entire thesis. Finally, the writer wishes to register his gratitude to his wife, Teresa, for typing the whole thesis.

## CHAPTER ONE

### INTRODUCTION

There are two types of nonlinearity in solid mechanics, namely, geometrical and physical nonlinearity (1). Geometrical nonlinearity deals with finite deformations, while physical nonlinearity deals with nonlinear stress-strain relations of the body. These two types of nonlinearity are independent of each other. Thus it follows that there are several types of problems in solid mechanics:

- (1) those linear both physically and geometrically (linear problems, elasticity),
- (2) those linear physically but nonlinear geometrically (nonlinear problems, elasticity),
- (3) those nonlinear physically but linear geometrically (nonlinear problems, e.g. plasticity with infinitesimal deformations),
- (4) those nonlinear both physically and geometrically (nonlinear problems, e.g. plasticity with finite deformations).

Nonlinear theories lead to nonlinear governing equations which immediately render classical methods of analysis inapplicable. Despite recent efforts on nonlinear behavior, only a few exact solutions to specific problems can be found; and these are

the most simple geometric shapes and boundary conditions. On the other hand, many nonlinear problems can be solved by numerical techniques which lead to approximate solutions.

The finite element method is one of these numerical techniques and has been found to be a powerful approach to stress analysis problems (2). Although early development of the method was primarily concerned with linear systems, the method has been extended to nonlinear problems by many researchers. The finite element formulation of geometrically nonlinear problems of elasticity has been generalized by N.D. Nathan (3). The study of physically nonlinear problems by the finite element method is the major study of present work.

The finite element formulation of plasticity was first presented by R.H. Gallagher and his colleagues (4). They followed the suggestions given by Mendelson and Manson (5), who proposed the so called initial (or thermal) strain method which is based on the idea of modifying the equilibrium equations of elasticity to compensate for the fact that the plastic strains do not cause any change in stress. Further developments in this category have been made by J.H. Argyris (6), L.H. Percy (7) and W.R. Jensen (8). This approach, however, cannot be used for perfectly plastic materials (9) or for a very small degree of hardening.

A few years later, G. Pope (10) introduced a different method known as the tangent modulus method, which is based on the incremental theory of plasticity, and solved the nonlinear

problem as a series of piece-wise linear systems. Subsequent contributions was made by T.L. Swedlow (11), S.F. Reys (12). Two years later, P.V. Marcal and I.P. King introduced a partial stiffness concept and make an elasto-plastic analysis of plane stress and plane strain problems as well as problems of axisymmetrically loaded bodies of revolution (13). At the same time, Y. Yamada (14) obtained an explicit expression of the incremental stress-strain relationship for the Prandtl-Reuss equations associated with the Von Mises yield criterion.

Two years later, a general formulation of plasticity was presented by O.C. Zienkiewicz and his colleagues (15), wherein an " initial stress " approach is proposed. This approach may be considered to save computing time, because a constant linear elastic matrix is used throughout the process. During the same year, Y. Yamada (16) extended his explicit elasto-plastic matrix to orthotropic materials on the basis of Hill's constitutive equations (17). More recently, G.C. Nayak and O.C. Zienkiewicz (18) have generalized problems in plasticity for various constitutive relations including strain softening, and have renamed the " initial stress method " the " residual force method ".

The present work, using an improved finite-element representation, deals with a detailed study of two-dimensional

elasto-plastic stress analysis problems with infinitesimal deformation. The computer programs for elastic analysis with the well-known constant strain triangular element were modified to include the elastoplastic analysis for the present study.

## CHAPTER TWO

### BASIC DEFINITIONS AND THEORIES OF ELASTICITY AND PLASTICITY

The theories of elasticity and plasticity deal with the systematic study of the state variables, stress, strain, and displacement in a solid body under the influence of external forces or prescribed displacements or both. In this chapter the basic equations of these theories will be reviewed for reference purposes and to establish the notation to be used.

For convenience rectangular cartesian coordinates  $X_i (X_1, X_2, X_3)$  will be employed for defining the three-dimensional space containing the body.

#### 1. Analysis of Stress

When a solid is under the action of external forces, it undergoes deformation and the effect of forces is transmitted throughout the body by interaction of material elements, giving rise to an internal force-stress field.

##### a. Stress Vector

Inside the body, isolate a surface of area  $A$  containing a point  $O$ . Fig.2-1. Due to external forces there will be some forces distributed over area  $A$ . These distributed forces will have a resultant force  $\underline{P}$  and a resultant moment  $\underline{M}$  at the point to  $O$ .

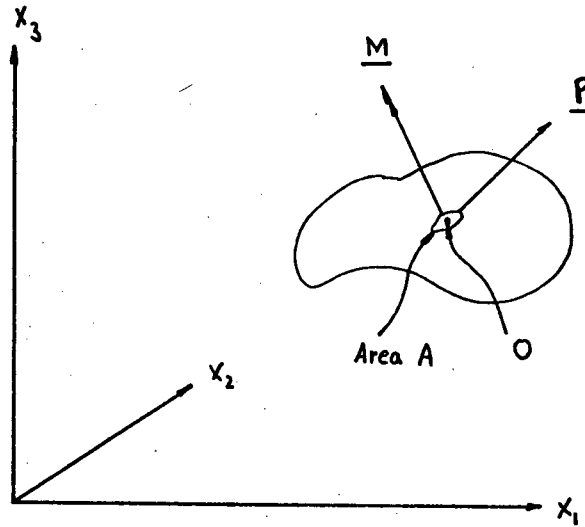


FIG.2-1 INTERNAL FORCES SYSTEM

After the concept of Love, the following limits are assumed to exist:

$$\lim_{A \rightarrow 0} \frac{M}{A} = 0, \quad (2-1a)$$

$$\lim_{A \rightarrow 0} \frac{P}{A} = \underline{t}. \quad (2-1b)$$

Where the limiting process is carried out so that  $O$  is always inside  $A$ .  $\underline{t}$  is a stress vector — force per unit area.

b. Stress Tensor

The stress vector  $\underline{t}(\underline{n})$  on an arbitrarily oriented surface with unit normal  $\underline{n}$  may be found once the stress vectors on each of three mutually perpendicular planes are known. The nine cartesian components of those three stress vectors form the stress tensor. (Fig.2-2):

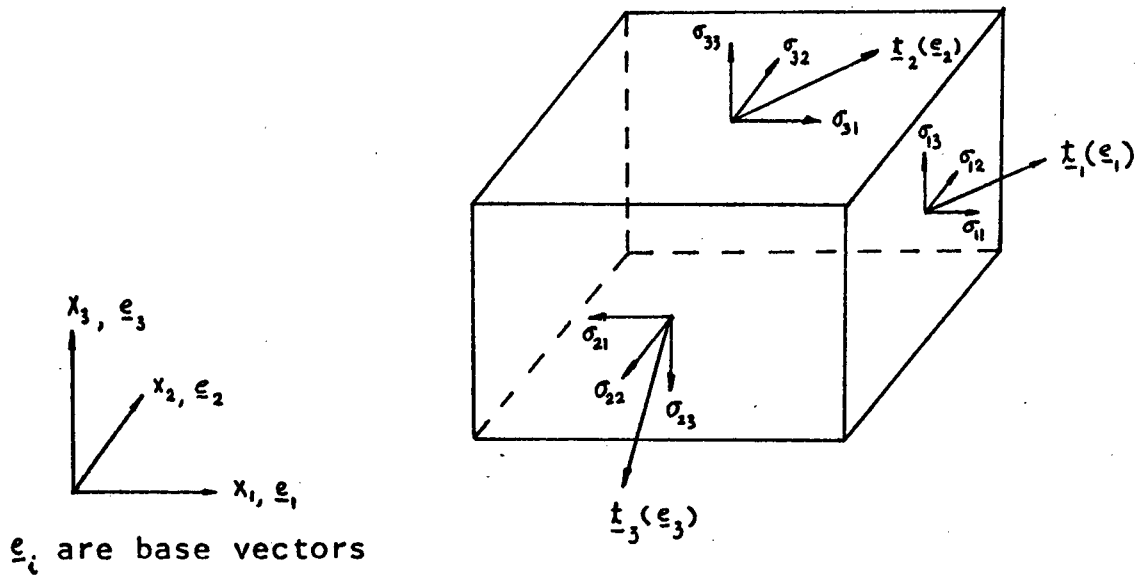


FIG.2-2 STRESS VECTORS AND POSITIVE STRESS COMPONENTS

$$\underline{t}_i = \sigma_{ij} \underline{e}_j \quad \text{(using summation convention on repeated indices)}$$

(2-2)

where

$$[\sigma_{ij}] = \begin{bmatrix} \sigma_{11} & \sigma_{12} & \sigma_{13} \\ \sigma_{21} & \sigma_{22} & \sigma_{23} \\ \sigma_{31} & \sigma_{32} & \sigma_{33} \end{bmatrix} \quad (2-3)$$



is called the stress tensor. The diagonal elements are called normal stresses and the off-diagonal elements, shear stresses. From (19) the stress tensor is symmetrical, i.e.  $\sigma_{ij} = \sigma_{ji}$ .

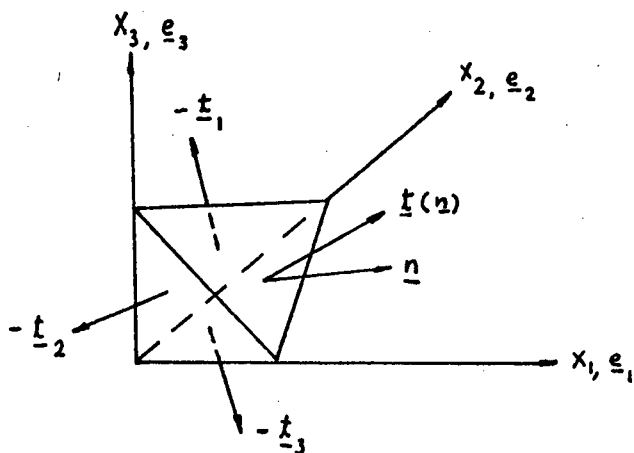


FIG.2-3 STRESS VECTORS ON A TETRAHEDRON

By considering Fig.2-3, we obtain Cauchy's formula:

$$\underline{t}(\underline{n}) = \underline{t}_i n_i, \quad (2-4)$$

or

$$\underline{t}(\underline{n}) = \sigma_{ij} n_i e_j, \quad (2-5)$$

which completely characterizes the state of stress at a point in terms of the nine cartesian stress components.

### c. Transformation of Coordinates

Suppose that two coordinate systems are available, Fig.2-4. A vector in space may be specified by giving its coordinates in either system, namely,  $X_i(x_1, x_2, x_3)$  or  $X'_k(x'_1, x'_2, x'_3)$ . Then the coordinates may be connected by the linear relations

$$X'_k = a_{ki} X_i \quad (2-6a)$$

$$X_i = a_{ik} X'_k \quad (2-6b)$$

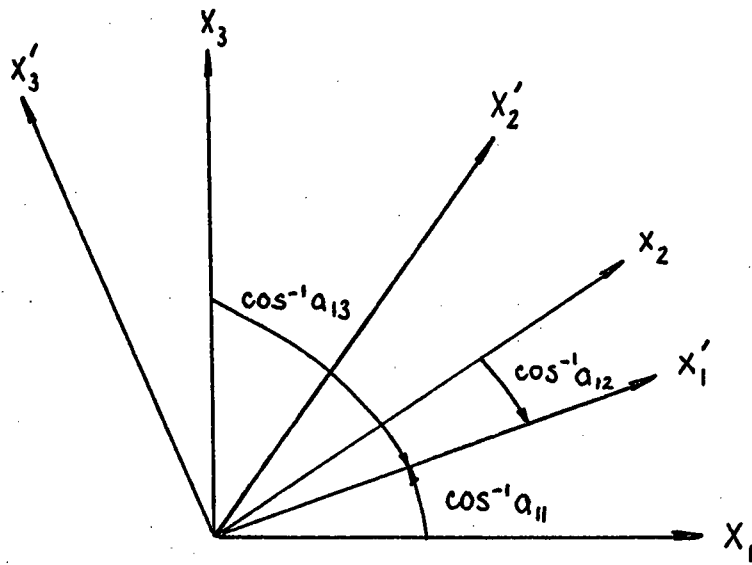


FIG.2-4 ROTATION OF COORDINATES

in which

$$[a_{ki}] = \begin{bmatrix} a_{11} & a_{12} & a_{13} \\ a_{21} & a_{22} & a_{23} \\ a_{31} & a_{32} & a_{33} \end{bmatrix}, \quad (2-7)$$

are the direction cosines of the  $X'_k$ -axis w.r.t. the  $X_i$ -axis as shown in Fig.2-4. Equations (2-6) define the transformation of a tensor of order one (20).

d. Stress Transformation Laws

Since the stress vector is a tensor of first order, Eq.(2-6) may be applied, i.e.

$$\underline{t}'_k(\underline{n}_k) = a_{ki} \underline{t}_i(\underline{n}_i),$$

$$\sigma'_{km} n_m = a_{ki} \sigma_{ij} n_j = a_{ki} a_{jm} \sigma_{ij} n_m,$$

$$\therefore (\sigma'_{km} - a_{ki} a_{jm} \sigma_{ij}) n_m = 0.$$

For arbitrary  $n_m$ ,

$$\sigma'_{km} = a_{ki} a_{jm} \sigma_{ij}. \quad (2-8a)$$

Similarly,

$$\sigma_{ij} = a_{ik} a_{jm} \sigma'_{km}. \quad (2-8b)$$

e. Equilibrium Equations

With regard to figure 2-2, we write the equilibrium equations in the  $X_1, X_2, X_3$  directions, and reduce to the equation:

$$\sigma_{ij,j} + F_i = 0, \quad (2-9)$$

which the stress tensor has to satisfy.

f. Principal Stresses, Principal Directions, Stress Invariants

We now seek a plane with direction  $\underline{n}$  for which the stress vector  $\underline{t}(\underline{n})$  is parallel to the outward normal  $\underline{n}$ . That is

$$\underline{t}(\underline{n}) - \sigma \underline{n} = 0$$

or 
$$(\sigma_{ij} - \sigma \delta_{ij}) n_j = 0. \quad (2-10)$$

where  $\delta_{ij}$  is called the Kronecker delta defined by

$$\delta_{ij} = \begin{cases} 1 & i = j \\ 0 & i \neq j \end{cases}.$$

Such a direction  $n_j$  is called a principal direction and the corresponding stress value  $\sigma$  is a principal stress. The characteristic equation for Eq.(2-10), which must be satisfied if these homogeneous equations in  $n_j$  are to have a solution, is

$$|\sigma_{ij} - \sigma \delta_{ij}| = 0, \quad (2-11)$$

which leads to the values of the principal stresses. For each value of the principal stress associated with  $n_i n_i = 1$ , a unit normal vector  $\underline{n}$  can be determined.

Expanding Eq.(2-11), yields

$$-\sigma^3 + I_1 \sigma^2 - I_2 \sigma + I_3 = 0,$$

where

$$I_1 = \sigma_{ii},$$

$$I_2 = \frac{1}{2} (\sigma_{ii} \sigma_{jj} - \sigma_{ij} \sigma_{ij}),$$

$$I_3 = |\sigma_{ij}|.$$

(2-12a)

If the reference axes coincide with the principal axes, then

$$\begin{aligned}
 I_1 &= \sigma_1 + \sigma_2 + \sigma_3, \\
 I_2 &= \sigma_1 \sigma_2 + \sigma_2 \sigma_3 + \sigma_3 \sigma_1, \\
 I_3 &= \sigma_1 \sigma_2 \sigma_3,
 \end{aligned}
 \tag{2-12b}$$

where  $\sigma_1, \sigma_2, \sigma_3$  are the principal stresses, the solutions of Eq.(2-11).  $I_1, I_2$  and  $I_3$  are called the first, second and third invariants of the stress tensor. It can be shown that one of the principal stress is the algebraically largest and another the algebraically smallest of those acting on any of the planes passing through the point in question.

g. Shearing Stresses

The resultant shearing stress component at a plane with unit normal vector  $\underline{n}$  is given by

$$\sigma_s^2 = \underline{t}(\underline{n}) \cdot \underline{t}(\underline{n}) - (\underline{t}(\underline{n}) \cdot \underline{n})^2$$

Let the principal axes be the coordinate axes, and:

$$\sigma_s^2 = \sigma_i^2 n_i^2 - (\sigma_i n_i)^2, \tag{2-13}$$

where  $\sigma_i$  is the principal stress. To find the extreme shear stresses, it is merely necessary to maximize Eq.(2-13) subject to the constraining relation

$$n_i n_i = 1. \tag{2-14}$$

The results are summary in Table 2-1. One of these values will, of course, be the largest shear stress acting on any plane passing through the point in question.

TABLE 2-1 MAX. SHEAR STRESS AND PRINCIPAL DIRECTION

n	n	n	corresponding $\sigma_s$
0	$\pm \frac{\sqrt{2}}{2}$	$\pm \frac{\sqrt{2}}{2}$	$\frac{1}{2}  \sigma_2 - \sigma_3 $
$\pm \frac{\sqrt{2}}{2}$	0	$\pm \frac{\sqrt{2}}{2}$	$\frac{1}{2}  \sigma_3 - \sigma_1 $
$\pm \frac{\sqrt{2}}{2}$	$\pm \frac{\sqrt{2}}{2}$	0	$\frac{1}{2}  \sigma_1 - \sigma_2 $

h. Stress Deviations, Deviatoric Stress Invariants

The stress tensor may be separated into two parts: one is spherical stress tensor  $P_{ij}$  (hydrostatic stress) which causes elastic dilatation, and the other is the deviatoric stress tensor  $S_{ij}$  (tangential stress) which causes elastic distortion and plastic strain.

$$\sigma_{ij} = S_{ij} + P_{ij}$$

where

$$P_{ij} = \frac{\sigma_{mm}}{3} \delta_{ij} \quad (2-15)$$

$$S_{ij} = \sigma_{ij} - \frac{\sigma_{mm}}{3} \delta_{ij} \quad (2-16)$$

The deviatoric stress invariants  $J_1, J_2, J_3$  are analogous to  $I_1, I_2, I_3$  Thus

$$J_1 = S_{ii} = 0$$

$$\begin{aligned} J_2 &= \frac{1}{2} (S_{ii} S_{jj} - S_{ij} S_{ij}) = \frac{1}{2} S_{ij} S_{ij} \\ &= \frac{1}{2} [S_x^2 + S_y^2 + S_z^2 + 2(S_{xy}^2 + S_{yz}^2 + S_{zx}^2)] \\ &= \frac{1}{2} (S_1^2 + S_2^2 + S_3^2) \quad (2-17) \\ &= \frac{1}{6} [(\sigma_x - \sigma_y)^2 + (\sigma_y - \sigma_z)^2 + (\sigma_z - \sigma_x)^2 + 6(\sigma_{xy}^2 + \sigma_{yz}^2 + \sigma_{zx}^2)] \\ &= \frac{1}{6} [(\sigma_1 - \sigma_2)^2 + (\sigma_2 - \sigma_3)^2 + (\sigma_3 - \sigma_1)^2] \end{aligned}$$

$$J_3 = |S_{ij}| = \frac{1}{3} S_{ij} S_{jk} S_{ki}$$

## II. Analysis of Strain

When forces are applied to a body, the position of any point of the body, in general, is changed. The displacement of a point is defined as the vector distance from the initial to the final location of the point. A body is considered to be strained whenever the relative position of points in the continuous body is altered.

### a. Strain Tensor

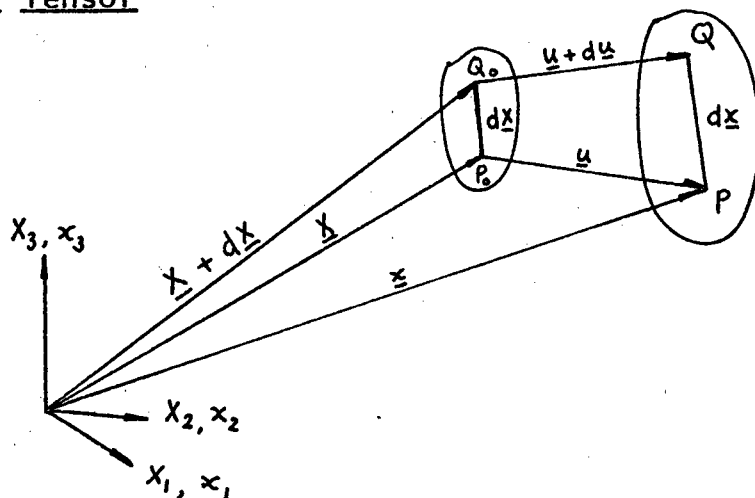


FIG.2-5 DISPLACEMENT OF NEIGHBORING POINTS

In Fig.2-5,  $P_0(x_1, x_2, x_3)$  is a material point in the undeformed body, and  $P(x_1, x_2, x_3)$  is the location of the same particle of material after deformation.  $Q_0(x_1 + dx_1, x_2 + dx_2, x_3 + dx_3)$  is a neighboring point of  $P_0$ , and its final position is  $Q(x_1 + dx_1, x_2 + dx_2, x_3 + dx_3)$ .  $\underline{u}$  is the displacement vector.

For homogeneous deformation, we can write

$$x_i = x_i (X_1, X_2, X_3), \quad (2-18a)$$

and

$$X_i = X_i (x_1, x_2, x_3), \quad (2-18b)$$

provided the Jacobian  $J = \left| \frac{\partial x_i}{\partial X_j} \right|$  does not vanish.

The square of the differential element of length between  $P_0$  and  $Q_0$  in the undeformed body is

$$(dX)^2 = d\underline{X} \cdot d\underline{X} = dX_i dX_i.$$

Similarly in the deformed body

$$(dx)^2 = d\underline{x} \cdot d\underline{x} = dx_i dx_i.$$

Form

$$\begin{aligned} (dx)^2 - (dX)^2 &= dx_i dx_i - dX_m dX_m \\ &= dx_i dx_j \delta_{ij} - X_{m,i} X_{m,j} dx_i dx_j \\ &= (\delta_{ij} - X_{m,i} X_{m,j}) dx_i dx_j. \end{aligned}$$

Alternatively, write

$$\begin{aligned} (dx)^2 - (dX)^2 &= dx_i dx_i - dX_m dX_m \\ &= x_{i,m} x_{i,n} dX_m dX_n - dX_m dX_n \delta_{mn} \\ &= (x_{i,m} x_{i,n} - \delta_{mn}) dX_m dX_n. \end{aligned}$$

We define the strain tensors

$$E_{ij} = \frac{1}{2} (\delta_{ij} - X_{m,i} X_{m,j}), \quad (2-19)$$

$$l_{ij} = \frac{1}{2} (x_{m,i} x_{m,j} - \delta_{ij}). \quad (2-20)$$

The strain tensor  $E_{ij}$  is called the Eulerian finite strain tensor, and  $l_{ij}$  is called the Lagrangian finite strain tensor. Both of them are symmetric.





$$\epsilon_{ij} = \epsilon_{ij} - \frac{\epsilon_{ii}}{3} \delta_{ij}. \quad (2-24)$$

c. Compatibility of Strain Components

The strain components cannot be arbitrarily prescribed and certain relations, called the compatibility conditions, must exist between them. The equations, for small strain, are given by (21)

$$\epsilon_{ij,kl} + \epsilon_{kl,ij} = \epsilon_{ik,jl} + \epsilon_{jl,ik}. \quad (2-25)$$

III. Field Equations in Elasticity

a. Generalized Hooke's Law

For a three dimensional state of stress, Cauchy generalized Hooke's law into the statement that each stress component is a linear function of all the strain components,

$$\sigma_{ij} = E_{ijkl} \epsilon_{kl}, \quad (2-26a)$$

where  $E_{ijkl}$  has the following properties:

$$\frac{\partial}{\partial x_m} (E_{ijkl}) = 0 \quad \text{for homogeneous materials,}$$

$$E'_{ijkl} = E_{ijkl} \quad \text{for isotropic materials.}$$

(The primed value being referred to a different set of coordinates)

b. Constitutive Equations

For homogeneous isotropic linear elastic materials, Eq.(2-26a) becomes ( 22)

or 
$$\sigma_{ij} = \lambda \epsilon_{ii} \delta_{ij} + 2G \epsilon_{ij}, \quad (2-26a)$$

$$\begin{cases} \sigma_{ij} = 3K \epsilon_{ij} \\ S_{ij} = 2G \epsilon_{ij} \end{cases}$$

Equation (2-26) can assume the alternative form

where 
$$\epsilon_{ij} = \frac{S_{ij}}{2G} + \delta_{ij} (1-2\nu) \frac{\sigma_{ii}}{3E}, \quad (2-26c)$$

$$E = \frac{G(3\lambda + 2G)}{\lambda + G} \quad \text{modulus of elasticity}$$

$$\nu = \frac{\lambda}{2(\lambda + G)} \quad \text{Poisson's ratio}$$

$$K = \frac{3\lambda + 2G}{3} \quad \text{bulk modulus}$$

$$= \frac{E}{3(1-2\nu)}$$

G and λ are the Lamé's constants.

c. Field Equations in Elasticity

The solution of a given problem in linear elasticity can proceed from the basic equations:

1. Equilibrium Equations

$$\sigma_{ij,j} + F_i = 0 \quad ; \quad (2-9)$$

2. Strain-displacement Equations

$$\epsilon_{ij} = \frac{1}{2} (u_{i,j} + u_{j,i}) \quad ; \quad (2-23)$$

3. Constitutive Equations

$$\sigma_{ij} = E_{ijkl} \epsilon_{kl} \quad . \quad (2-26)$$

These fifteen equations are the governing equations for the fifteen unknown state variables  $\sigma_{ij}$ ,  $\epsilon_{ij}$ ,  $u_i$ . They must be satisfied at all point inside an elastic solid in static equilibrium. Together with the boundary conditions:

$$\sigma_{ij} n_j = T_i \text{ prescribed on } S_\sigma,$$

$$u_i = \mu_i \text{ prescribed on } S_\mu.$$

The solution is possible and unique. (23)

#### IV. Field Equations in Plasticity

##### a. Yield Theory

##### 1. Yield Surface

The yield surface is defined as the surface in stress space, with stress components as coordinates, within which the stress vector may change without any plastic-strain increment; stress increments beginning from points in the surface, if directed toward the exterior, imply plastic strain increments.

##### 2. Initial Yield Surface

For isotropic plasticity, the initial yield surface must be independent of the orientation of the reference axes. By choosing the axes of the principal stresses as the reference axes, the initial yield surface may be expressed in terms of the principal stresses and represented by a surface in a stress space with  $\sigma_1$ ,  $\sigma_2$ ,  $\sigma_3$  as coordinate axes. Thus the initial yield function may appear as

$$f(\sigma_1, \sigma_2, \sigma_3) = 0.$$

Furthermore, experiment indicates that the hydrostatic pressure has no effect on the plastic deformation. Hence the initial yield condition may be expressed in

terms of the deviatoric stress invariants in the form

$$f(J_2, J_3) = 0.$$

Two simple yield conditions for the initial yield of isotropic material which have provided highly useful descriptions of many real materials are discussed in the following section.

(1). Tresca Yield Condition (Maximum Shear Theory)

This hypothesis is based on the assumption that yield occurs when the maximum shear stress reaches a limiting value. In view of the results given in Table 2-1, a complete mathematical description of the Tresca condition is given in Table 2-2, and shown in Fig. 2-6.

TABLE 2-2

Stress State	Tresca Condition
$\sigma_1 < \sigma_2 < \sigma_3$	$\sigma_3 - \sigma_1 = \sigma_0$
$\sigma_3 < \sigma_2 < \sigma_1$	$\sigma_1 - \sigma_3 = \sigma_0$
$\sigma_1 < \sigma_3 < \sigma_2$	$\sigma_2 - \sigma_1 = \sigma_0$
$\sigma_2 < \sigma_3 < \sigma_1$	$\sigma_1 - \sigma_2 = \sigma_0$
$\sigma_2 < \sigma_1 < \sigma_3$	$\sigma_3 - \sigma_2 = \sigma_0$
$\sigma_3 < \sigma_1 < \sigma_2$	$\sigma_2 - \sigma_3 = \sigma_0$

where  $\sigma_0$  = yield stress for simple tension.

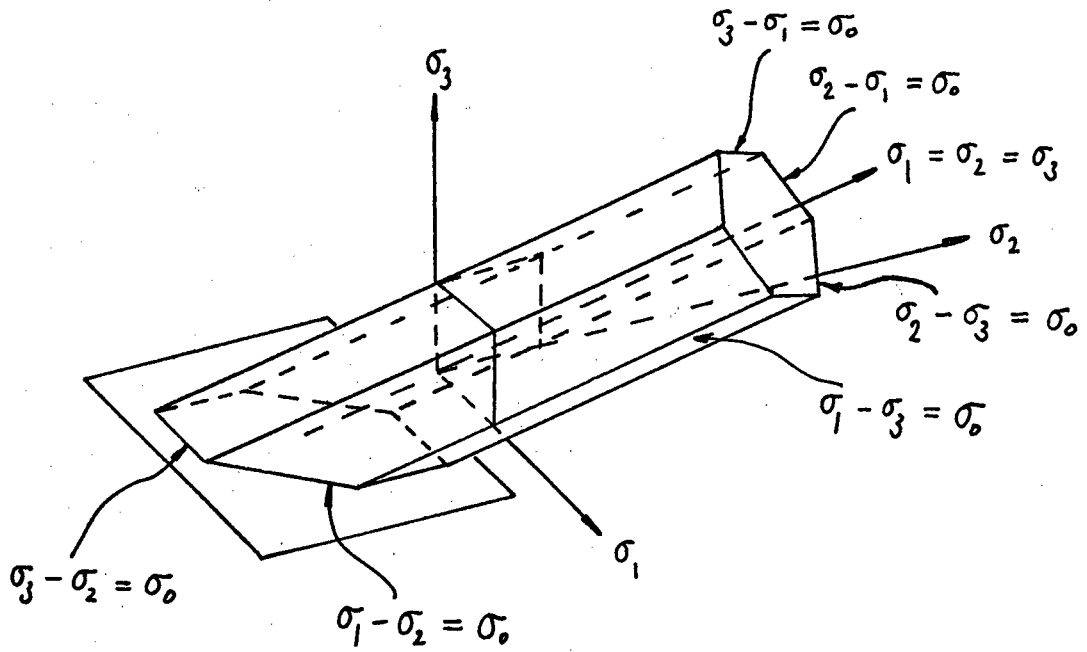


FIG. 2-6 TRESCA YIELD SURFACE IN PRINCIPAL STRESS SPACE

The Tresca yield condition given by Table 2-2 can be represented by

$$f = [(\sigma_1 - \sigma_2)^2 - \sigma_0^2][(\sigma_2 - \sigma_3)^2 - \sigma_0^2][(\sigma_3 - \sigma_1)^2 - \sigma_0^2]$$

or

$$f = 4J_2^3 - 27J_3^2 - 9\sigma_0^2 J_2^2 + 6\sigma_0^4 J_2 - \sigma_0^6 = 0 \quad (2-27)$$

where  $J_2, J_3$  are the deviatoric stress invariants.

(2). Von Mises Yield Condition (Distortion Energy Theory)

Von Mises hypothesised that yielding occurs when the second deviatoric stress invariant attains a prescribed value  $k^2$ . For the uniaxial stress state  $k^2 = \frac{\sigma_0^2}{3}$ . Then

$$f = J_2 - \frac{\sigma_0^2}{3} = 0. \quad (2-28)$$

Fig. 2-7 shows the geometrical meaning of the Von Mises condition.

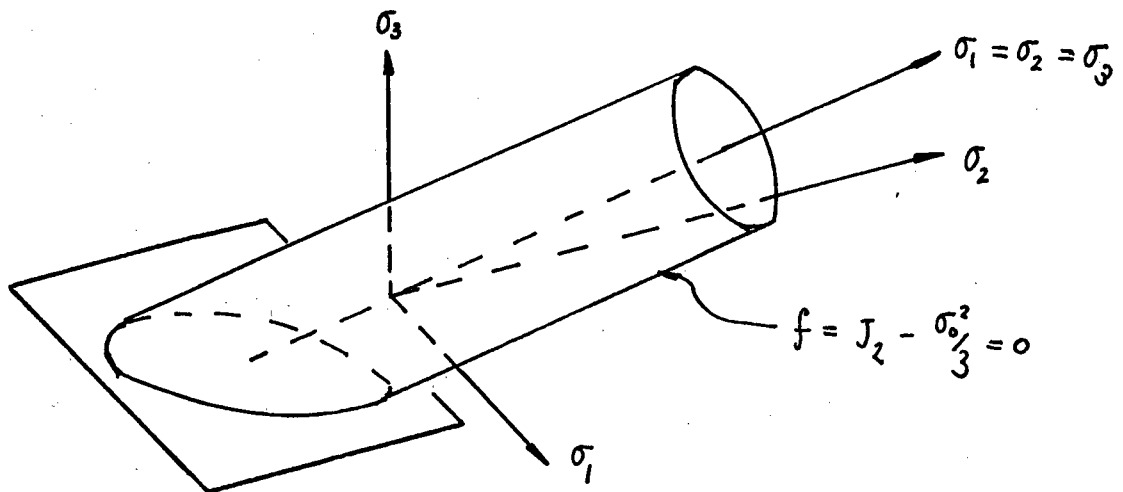


FIG. 2-7. VON MISES YIELD SURFACE IN PRINCIPAL STRESS SPACE



### 3. Subsequent Yield Surface

Continued loading beyond the initial yield surface leads to plastic deformation which may be accompanied by changes in both size and shape of the yield surface. For perfect plasticity the yield surface does not change during plastic deformation and the initial yield surface remains valid. For isotropic hardening, however, the size of the yield surface increases, but the shape remains the same during loading. To take into account such changes it is necessary to modify the initial yield surface and to define the subsequent yield surface, also known as the loading surface. A general form for the loading surface is given by (24)

$$f(\sigma_{ij}, \epsilon_{ij}^p, \kappa) = 0, \quad (2-29)$$

Which depends not only upon the stresses  $\sigma_{ij}$ , but also upon the plastic strains  $\epsilon_{ij}^p$  and the work hardening characteristics represented by the parameter  $\kappa$ . Differentiating  $f=0$  by the chain rule of calculus, we obtain

$$df = \frac{\partial f}{\partial \sigma_{ij}} d\sigma_{ij} + \frac{\partial f}{\partial \epsilon_{ij}^p} d\epsilon_{ij}^p + \frac{\partial f}{\partial \kappa} d\kappa,$$

where  $df$ ,  $d\sigma_{ij}$ , etc. represent time differentials.

If  $f=0$  and  $df < 0$  a condition leading to an elastic state is implied, and it must follow that  $d\varepsilon_{ij}^p = dK = 0$ . Thus

$$f = 0, \quad \frac{\partial f}{\partial \sigma_{ij}} d\sigma_{ij} < 0 \quad \text{is defined as "unloading"}$$

$$f = 0, \quad \frac{\partial f}{\partial \sigma_{ij}} d\sigma_{ij} = 0 \quad \text{is defined as "neutral loading", since it implies that the stress-point remains on the initial yield surface.}$$

$$f = 0, \quad \frac{\partial f}{\partial \sigma_{ij}} d\sigma_{ij} > 0 \quad \text{is defined as "loading", since it implies that the stress-point is moving outward from the current yield surface.}$$

For perfectly plastic materials plastic flow occurs

for

$$f = 0, \quad \frac{\partial f}{\partial \sigma_{ij}} d\sigma_{ij} = 0,$$

and the case

$$f = 0, \quad \frac{\partial f}{\partial \sigma_{ij}} d\sigma_{ij} > 0 \quad \text{does not exist.}$$

b. Constitutive Equation: -Plastic-flow rule of incremental type

Based on the following assumptions:

1. isotropic elasto-perfectly plastic materials,
2. the principal axes of stress and plastic strain increment coincide,

$$3. \quad d\varepsilon_{ij} = d\varepsilon_{ij}^e + d\varepsilon_{ij}^p, \quad (2-30)$$

$$4. \quad d\varepsilon_{ij}^e = \frac{d\sigma_{ij}}{2G} + (1-2\nu)\delta_{ij} \frac{d\sigma_{ij}}{3E}, \quad (2-31)$$

$$5. \quad d\varepsilon_{ii}^p = 0, \quad (2-32)$$

Reuss extended a proposal of Prandtl to say that the plastic strain increments  $d\varepsilon_{ij}^P$  are related to the stress deviator components  $S_{ij}$  by

$$d\varepsilon_{ij}^P = d\lambda S_{ij} \quad (2-33)$$

where  $d\lambda$  is the proportionality factor, which may change during loading.

For work-hardening materials associated with the Von Mises yield condition, it is useful to define the equivalent stress  $\bar{\sigma}$  and equivalent plastic strain increment  $\bar{d\varepsilon}^P$  as

$$\bar{\sigma} = \sqrt{\frac{3}{2} S_{ij} S_{ij}} \quad , \quad (2-34)$$

and

$$\bar{d\varepsilon}^P = \sqrt{\frac{2}{3} d\varepsilon_{ij}^P d\varepsilon_{ij}^P} \quad . \quad (2-35)$$

Then the Prandtl-Reuss flow rule becomes

$$d\varepsilon_{ij}^P = \frac{3 \bar{d\varepsilon}^P}{2 \bar{\sigma}} S_{ij} \quad , \quad (2-36)$$

with

$$d\lambda = \frac{3 \bar{d\varepsilon}^P}{2 \bar{\sigma}} \quad . \quad (2-37)$$

The plastic work increment is defined by (25)

$$dW_p = \sigma_{ij} d\varepsilon_{ij}^P = S_{ij} d\varepsilon_{ij}^P$$

in which  $d\varepsilon_{ii}^P = 0$  has been introduced. Furthermore, if the same material follows the Prandtl-Reuss flow rule, the plastic work increment may be expressed as

$$dW_p = \bar{\sigma} d\bar{\varepsilon}^P,$$

and the Prandtl-Reuss equation becomes

$$d\varepsilon_{ij}^P = \frac{3dW_p}{2\bar{\sigma}^2} S_{ij}.$$

By using the work-hardening hypothesis discussed in (26), the Prandtl-Reuss equation may be written as

$$d\varepsilon_{ij}^P = \frac{3d\bar{\sigma}}{2\bar{\sigma}H'} S_{ij}, \quad (2-38)$$

where

$$H' = \frac{d\bar{\sigma}}{d\bar{\varepsilon}^P}, \quad (2-39)$$

corresponds to the slope of the equivalent stress  $\bar{\sigma}$  versus equivalent plastic strain  $\int d\bar{\varepsilon}^P$  curve. Substituting Eq.(2-38) into Eq.(2-30), in view of Eq.(2-31), leads to

$$d\varepsilon_{ij} = \frac{dS_{ij}}{2G} + \frac{(1-2\nu)}{E} \delta_{ij} \frac{d\sigma_{ii}}{3} + \frac{3d\bar{\sigma}}{2\bar{\sigma}H'} S_{ij}, \quad d\bar{\sigma} \geq 0 \quad (2-40)$$

For unloading where  $d\bar{\sigma} < 0$  the elastic strain is the only applicable term and

$$d\varepsilon_{ij} = \frac{dS_{ij}}{2G} + \frac{(1-2\nu)}{E} \delta_{ij} \frac{d\sigma_{ii}}{3} \quad (2-41)$$

writing Eq. (2-40) in decomposite form will lead to Hill's complete stress-strain equation (27)

$$\begin{cases} d\varepsilon_{ij} = \frac{dS_{ij}}{2G} + \frac{3d\bar{\sigma}}{2\bar{\sigma}H'} S_{ij}, & d\bar{\sigma} \geq 0 \\ d\varepsilon_{ii} = \frac{(1-2\nu)}{E} d\sigma_{ii}, \end{cases} \quad (2-42)$$

in which  $d\varepsilon_{ii}^p = 0$  has been introduced.

A general equation for determining the plastic strain-stress relation for any yield condition was proposed by D.C. Drucker. Based on his definition of work-hardening materials (28), Drucker jumped one step beyond the classical treatment, and showed that, for these materials, the plastic strain increment vector must be normal to the yield or loading surface at a smooth point on that surface, and must lie between adjacent normals at a corner point. i.e. (29)

$$d\varepsilon_{ij}^p = d\lambda \frac{\partial f}{\partial \sigma_{ij}} \quad (2-43)$$

Eq.(2-43) is also called the normality principle of plasticity.

c. Field Equations In Plasticity

1. Equilibrium Equations

$$d\sigma_{ij,j} + dF_i = 0 \quad ; \quad (2-9)$$

2. Strain-displacement Equations

$$d\varepsilon_{ij} = \frac{1}{2} (du_{i,j} + du_{j,i}), \quad (2-23)$$

$$d\varepsilon_{ij} = d\varepsilon_{ij}^e + d\varepsilon_{ij}^p \quad ; \quad (2-30)$$

3. Constitutive Equations

$$d\varepsilon_{ij}^p = d\lambda \frac{\partial f}{\partial \sigma_{ij}}, \quad (2-43)$$

$$d\varepsilon_{ij}^e = \frac{dS_{ij}}{2G} + (1-2\nu)S_{ij} \frac{d\sigma_{ii}}{3E}, \quad (2-31)$$

where  $f(\sigma_{ij}, \varepsilon_{ij}^p, \kappa) = 0$  defines the yield surface.

4. Boundary Conditions

$$d\sigma_{ij}n_j = dT_i \text{ prescribed on } S_\sigma,$$

$$du_i = \bar{u}_i \text{ prescribed on } S_u.$$

It is seen that the plasticity problem is defined in a manner similar to an elasticity problem of the infinitesimal deformation theory, except for the stress-strain relations. Thus, once the problem in flow theory has been formulated, problems of plasticity can be analysed by integrating the resulting relations along the prescribed loading path.

### CHAPTER THREE

#### FINITE ELEMENT METHOD

The basis of and the formulation of the finite element procedure will be reviewed here to establish the approach and the notation used in these studies. This will be done for the linear elastic case, and the extension to the plasticity problem will be made in the next chapter.

It seems redundant to mention that the finite element method has been found to be a powerful approach to stress analysis of boundary value problems. Part of its advantage stems from its ability to take care of the irregular shapes of boundary and mixed boundary conditions.

The basic concept of the finite element method is that a continuum can be decomposed into a finite number of regions (elements), in each of which the behavior is represented by a separate field. In order to guarantee the convergence of the finite element solution to the exact values, these fields are so chosen that they satisfy the completeness requirement and, if possible, inter-element boundaries are made compatible (the "conformity" condition). Oliveira proved that, convergence of the finite element solution requires only the preservation of



correct rigid body and constant strain modes; ie. that compatibility could be relaxed if the completeness condition is satisfied (30). This remarkable result makes application of the finite element method to plate bending problems, for example, much simpler.

The finite element method may be interpreted as a particular case of Ritz's method associated with a variational principle in continuum mechanics. From the different variational principles in solid mechanics, it is possible to derive numerous finite element models which may lead to either a stiffness method (principle of minimum potential energy), a flexibility method (principle of minimum complimentary energy) or a mixed method (31).

### I. Variational Principles

Variational principles have made a great contribution to the development of stress analysis by the finite element method: for example, in deriving a finite element formulation, in providing the physical interpretation of the approximate governing equations thus derived, and most notably, in establishing convergence proofs and bounds formulae.

a. Principle of Minimum Potential Energy

Consider a continuous and sufficiently differentiable displacement field  $u_i^*$  such that

$$u_i^* = \text{prescribed displacements on } S_u,$$

$$\epsilon_{ij}^* = \frac{1}{2} (u_{i,j}^* + u_{j,i}^*),$$

and

$$\sigma_{ij}^* = E_{ijkl} \epsilon_{kl}^*.$$

Note that the stress field  $\sigma_{ij}^*$  is not necessarily in equilibrium, i.e.

$$\sigma_{ij,j}^* + F_i = 0,$$

and

$$\sigma_{ij}^* n_j = T_i \text{ on } S_\sigma \text{ may not be true.}$$

Form

$$\int_{S_\sigma} T_i (u_i^* - u_i) ds + \int_V F_i (u_i^* - u_i) dv = \int_{S_\sigma} \sigma_{ij} n_j (u_i^* - u_i) ds + \int_V F_i (u_i^* - u_i) dv$$

(equilibrium requirement at surface)

$$= \int_V [\sigma_{ij} (u_i^* - u_i)]_{,j} dv + \int_V F_i (u_i^* - u_i) dv$$

(divergence theorem)

$$= \int_V (\sigma_{ij,j} + F_i) (u_i^* - u_i) dv + \int_V \sigma_{ij} (u_{ij}^* - u_{ij}) dv$$

Noting that (for equilibrium)

$$\sigma_{ij,j} + F_i = 0,$$

$$\sigma_{ij} = \sigma_{ji},$$

and that

$$\sigma_{ij} (u_{i,j}^* - u_{i,j}) = \frac{1}{2} (\sigma_{ij} u_{i,j}^* + \sigma_{ji} u_{j,i}^*) - \frac{1}{2} (\sigma_{ij} u_{i,j} + \sigma_{ji} u_{j,i})$$

(dummy subscripts)

$$= \sigma_{ij} \left[ \frac{1}{2} (u_{i,j}^* + u_{j,i}^*) - \frac{1}{2} (u_{i,j} + u_{j,i}) \right]$$

(moment equilibrium)

$$= \sigma_{ij} (\varepsilon_{ij}^* - \varepsilon_{ij})$$

(strain-displacement relations)

thus Eq.(3-1) may be written as

$$\begin{aligned} \int_{S_\sigma} T_i (u_i^* - u_i) ds + \int_V F_i (u_i^* - u_i) dV &= \int_V \sigma_{ij} (\varepsilon_{ij}^* - \varepsilon_{ij}) dV \\ &= \int_V \left[ \frac{1}{2} (\sigma_{ij}^* \varepsilon_{ij}^* - \sigma_{ij} \varepsilon_{ij}) + \frac{1}{2} (\sigma_{ij}^* \varepsilon_{ij} - \sigma_{ij} \varepsilon_{ij}^*) \right. \\ &\quad \left. - \frac{1}{2} (\varepsilon_{ij}^* - \varepsilon_{ij}) (\sigma_{ij}^* - \sigma_{ij}) \right] dV. \end{aligned}$$

Noting that

(3-2)

$$\int_V \frac{1}{2} (\varepsilon_{ij}^* - \varepsilon_{ij}) (\sigma_{ij}^* - \sigma_{ij}) dV = \int_V \frac{1}{2} (\varepsilon_{ij}^* - \varepsilon_{ij}) E_{ijkl} (\varepsilon_{kl}^* - \varepsilon_{kl}) \geq 0$$

since  $E_{ijkl}$  is positive definite, and that

$$\sigma_{ij}^* \varepsilon_{ij} = E_{ijkl} \varepsilon_{kl}^* \varepsilon_{ij} = \sigma_{kl}^* \varepsilon_{kl} = \sigma_{ij} \varepsilon_{ij}^*$$

because all the subscripts are dummy, Eq(3-2) becomes

$$\int_{S_\sigma} T_i (u_i^* - u_i) ds + \int_V F_i (u_i^* - u_i) dV \leq \int_V \frac{1}{2} (\sigma_{ij}^* \varepsilon_{ij}^* - \sigma_{ij} \varepsilon_{ij}) dV,$$

or

$$-\int_{S_\sigma} T_i u_i^* ds - \int_V F_i u_i^* dV + \int_V \frac{1}{2} \sigma_{ij}^* \varepsilon_{ij}^* \geq -\int_{S_\sigma} T_i u_i dV - \int_V F_i u_i dV + \int_V \frac{1}{2} \sigma_{ij} \varepsilon_{ij} dV. \quad (3-3)$$

Thus the minimum potential energy principle states that: Of all the kinematically admissible displacement fields, the actual solution i.e. the one which not only satisfies the compatibility conditions but which also corresponds to a stress field which satisfies the equilibrium condition, is distinguished by the stationary value of the corresponding total potential energy. The solution can be shown to be unique for linear systems.

II. Formulation of Finite Element Method by  
The Principle of Minimum Potential Energy

In formulating the finite element method, the displacement field is represented by interpolation functions together with generalized displacements at a finite number of nodal points in each element. To fulfill the general completeness requirement, the field components and all their derivatives, of order not higher than the highest derivative entering the energy density expression must be able to take up any constant (non-zero) value within the element. It follows that if  $p$  is the order of the highest derivative appearing in the energy expression (for example,  $p=2$  for plate bending problems), then it is only necessary that the interpolation function must contain a complete polynomial up to the  $p^{\text{th}}$  degree, all the terms of which have independent arbitrary coefficients. The terms of higher degree may be allowed to vanish whatever values are taken by those coefficients. For example, O.C. Zienkiewicz has omitted some fourth-order terms from a complete fourth-order polynomial for a rectangular plate bending element. The interpolation functions he uses satisfy the above requirements for the plate bending problem and can yield constant values for deflection, slopes and curvatures if the nodal variables are suitably prescribed. In other words, the

parameters of the polynomial are entirely defined by the generalized displacements. In matrix form the assumed displacement may be written as

$$\underline{u} = \underline{A} \underline{s} \quad (3-4)$$

where  $\underline{u}$  = displacement column matrix,  
 $\underline{s}$  = nodal displacement column matrix,  
 $\underline{A}$  = shape function matrix.

The corresponding strain column matrix is

$$\underline{\epsilon} = \underline{L} \underline{u} \quad (3-5)$$

where  $\underline{L}$  is the differential operators matrix.

The corresponding stress column matrix is

$$\underline{\sigma} = \underline{D} \underline{\epsilon} \quad (3-6)$$

where  $\underline{D}$  is the elastic constant matrix.

The total potential energy functional for any elastic solid is given by

$$V_p = - \int_{S_f} T_i u_i ds - \int_V F_i u_i dV + \int_V \frac{1}{2} \sigma_{ij} \epsilon_{ij} dV \quad (3-7)$$

If the body is divided into a finite number of discrete elements  $V_n$ , then

$$V_p = \sum_n \left[ - \int_{S_{\sigma n}} T_i u_i ds - \int_{V_n} F_i u_i dV + \int_{V_n} \frac{1}{2} \sigma_{ij} \epsilon_{ij} dV \right], \quad (3-7a)$$

or in matrix form

$$V_p = \sum_n \left[ - \int_{S_{\sigma n}} \underline{u}^T \underline{I} ds - \int_{V_n} \underline{u}^T \underline{F} dV + \int_{V_n} \frac{1}{2} \underline{\sigma}^T \underline{\epsilon} dV \right]. \quad (3-7b)$$

Substituting equations (3-4), (3-5), and (3-6) into (3-7b), leads to

$$\begin{aligned}
 V_p &= \sum_n \left[ - \int_{S_{\sigma_n}} \underline{s}^T \underline{A}^T \underline{I} \, dS - \int_{V_n} \underline{s}^T \underline{A}^T \underline{E} \, dV + \int_{V_n} \frac{1}{2} (\underline{L} \underline{A} \underline{s})^T \underline{D} (\underline{L} \underline{A} \underline{s}) \, dV \right] \\
 &= \sum_n \left[ - \underline{s}^T \left\{ \int_{S_{\sigma_n}} \underline{A}^T \underline{I} \, dS + \int_{V_n} \underline{A}^T \underline{E} \, dV \right\} + \frac{1}{2} \underline{s}^T \left\{ \int_{V_n} (\underline{L} \underline{A})^T \underline{D} (\underline{L} \underline{A}) \, dV \right\} \underline{s} \right] \\
 &= \sum_n \left[ - \underline{s}^T \underline{S} + \frac{1}{2} \underline{s}^T \underline{k} \underline{s} \right]
 \end{aligned} \tag{3-8}$$

where

$$\underline{k} = \int_{V_n} (\underline{L} \underline{A})^T \underline{D} (\underline{L} \underline{A}) \, dV \tag{3-9}$$

= member stiffness matrix

$$\underline{S} = \int_{S_{\sigma_n}} \underline{A}^T \underline{I} \, dS + \int_{V_n} \underline{A}^T \underline{E} \, dV \tag{3-10}$$

= nodal force column matrix

The nodal displacements  $\underline{S}$  for different elements are not completely independent; A transformation is needed to relate the element nodal displacements to the independent generalized global displacements. Then the compatibility equations of the assembled structure are written in matrix form as

$$\underline{S} = \underline{a} \underline{r} \quad (3-11)$$

where  $\underline{a}$  = compatibility transformation matrix,  
 $\underline{r}$  = global displacement column matrix.

Substituting Eq.(3-11) into (3-8), yields

$$\begin{aligned} V_p &= -\underline{r}^T \left( \sum_n \underline{a}^T \underline{S} \right) + \frac{1}{2} \underline{r}^T \left( \sum_n \underline{a}^T \underline{k} \underline{a} \right) \underline{r} \\ &= -\underline{r}^T \underline{R} + \frac{1}{2} \underline{r}^T \underline{K} \underline{r} \end{aligned} \quad (3-12)$$

where

$$\underline{K} = \sum_n \underline{a}^T \underline{k} \underline{a} \quad (3-13)$$

= global stiffness matrix

$$\underline{R} = \sum_n \underline{a}^T \underline{S} \quad (3-14)$$

= global force column matrix.

The principle of minimum potential energy requires that

$\delta V_p = 0$ , i.e.

$$\frac{\partial V_p}{\partial \underline{r}} \delta \underline{r} = (-\underline{R} + \underline{K} \underline{r}) \delta \underline{r} = 0.$$

For arbitrary  $\delta \underline{r}$

$$\underline{K} \underline{r} = \underline{R}. \quad (3-15)$$

Thus, for a given force vector  $\underline{R}$  the corresponding displacement vector  $\underline{r}$  can be obtained by the inversion of  $\underline{K}$  as

$$\underline{r} = \underline{K}^{-1} \underline{R}, \quad (3-16)$$

and the nodal displacements, corresponding strain and stress within each element may be found by equations (3-11), (3-5) and (3-6).



## CHAPTER FOUR

### FORMULATION OF ELASTO-PLASTIC PROBLEMS

#### I. General Considerations

Plastic theory is often associated with large deformations, but a plastic deformation analysis involving large deformations is complicated both by geometric nonlinearities and by anisotropic hardening. Moreover, the lack of experimental support for elasto-plastic computational results in the range of infinitesimal deformation makes an excursion into the field of large deformation plasticity a precarious enterprise. Hence, in the present study attention will be focused on plasticity with infinitesimal deformations.

The finite element displacement method is preferred, even though the force method might be better in a philosophical sense (32).

The method of incremental loading is frequently employed in the analysis of a path-dependent process such as plastic deformation. By this method the complete nonlinear response of the solid body is generated as a sequence of piece-wise linear systems, Fig.4-1. If  $\Delta R$  (a typical load increment) is taken sufficiently small, then the approximate state is reasonably acceptable, even though some error  $\epsilon$  will inevitably enter each step of the process. This error, however, can be reduced by means of a numerical iteration procedure such as the well-known Newton-Raphson method or the modified Newton-Raphson method, Fig.4-2.

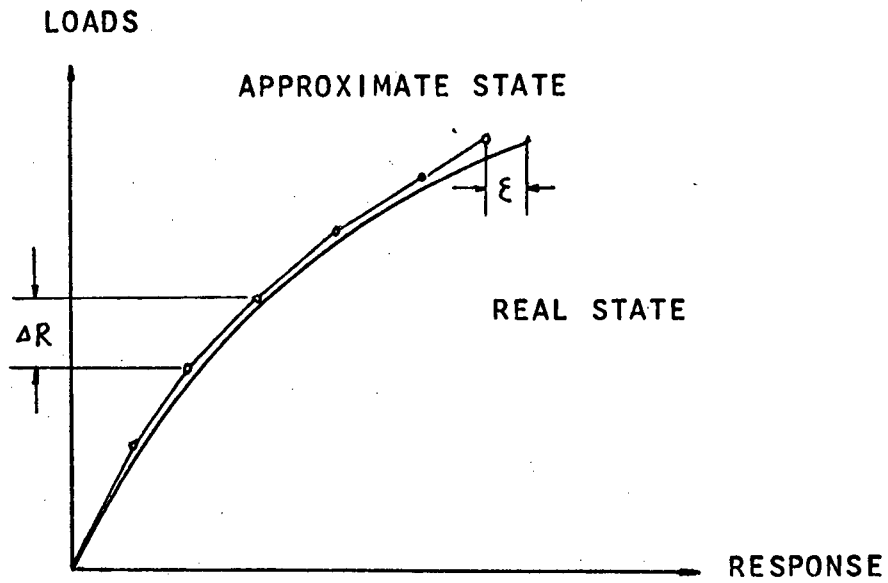
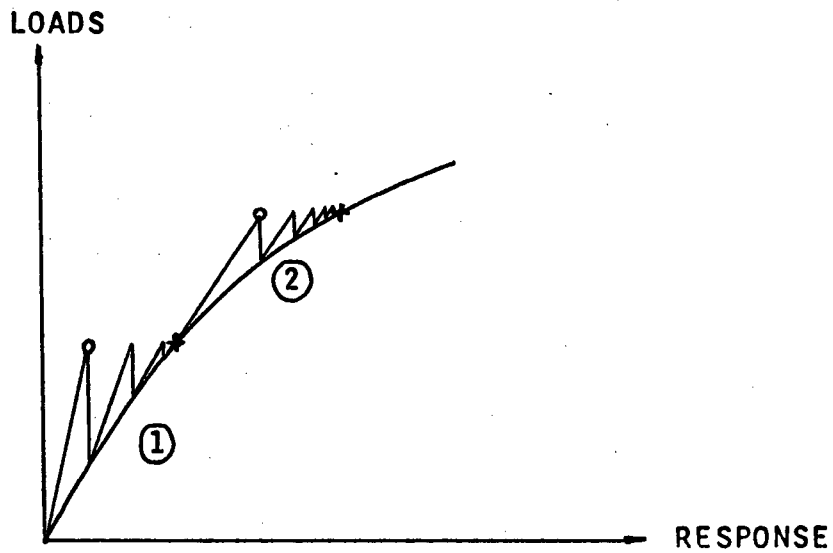


FIG.4-1 THE INCREMENTAL LOADING PROCESS



- o - incremental loading
- x - 1 corrected by Newton-Raphson method
- x - 2 corrected by Modified Newton-Raphson method

FIG.4-2 A COMBINATION OF THE LOAD INCREMENT AND NEWTON-RAPHSON (OR MADIFIED NEWTON-RAPHSON) METHOD

## II. Generalized Incremental Equilibrium Equation

During each load increment, the equilibrium equations can be obtained by following the procedures given in chapter three.

Let 
$$\underline{\Delta \mu} = \underline{A} \underline{\Delta S}, \quad (4-1)$$

$$\underline{\Delta \varepsilon} = \underline{L} \underline{\Delta \mu}, \quad (4-2)$$

where  $\underline{\Delta \mu}$  = a column vector of displacement increments  
 $\underline{\Delta S}$  = a column vector of nodal displacement increments  
 $\underline{\Delta \varepsilon}$  = a column vector of strain increments.

For isotropic materials we assumed the incremental stress and strain are related by Hooke's law in the elastic region and by the Prandtl-Reuss (or Drucker) definition during loading in the plastic region, i.e.

$$\underline{\Delta \sigma} = \underline{D}_{ep}'' \underline{\Delta \varepsilon}. \quad (4-3)$$

The matrix  $\underline{D}_{ep}''$  contains only the material properties of an elastic element, i.e.

$$\underline{D}_{ep}'' = \underline{D},$$

but in the plastic region it depends, in addition, on the current state of stress and hardening of the element, i.e.

$$\underline{D}_{ep}'' = \underline{D}_{ep}' \quad (\text{see next section}).$$

A variational formulation for the materials of elasto-

plastic behavior assumes a stationary value of functional (see appendix)

$$V^* = \sum_n \left[ - \int_{S_{\sigma_n}} \underline{\Delta T}^T \underline{\Delta u} dS - \int_{V_n} \underline{\Delta F}^T \underline{\Delta u} dV + \int_{V_n} \frac{1}{2} \underline{\Delta \sigma}^T \underline{\Delta \xi} dV \right], \quad (4-4)$$

where  $\underline{\Delta T}$  = a column vector of surface traction increments,  
 $\underline{\Delta F}$  = a column vector of body force increments.

By introducing the "global stiffness matrix":

$$\underline{K} = \underline{a}^T \sum_n \left[ \int_{V_n} (\underline{L}A)^T \underline{D}_{ep}^{**} (\underline{L}A) dV \right] \underline{a}, \quad (4-5)$$

the "global force vector":

$$\underline{\Delta R} = \underline{a}^T \sum_n \left[ \int_{S_{\sigma_n}} \underline{\Delta T}^T A dS + \int_{V_n} \underline{\Delta F}^T A dV \right], \quad (4-6)$$

and the compatibility equations

$$\underline{\Delta s} = \underline{a} \underline{\Delta r}, \quad (4-7)$$

then Eq.(4-4) becomes

$$V^* = - \underline{\Delta r}^T \underline{\Delta R} + \frac{1}{2} \underline{\Delta r}^T \underline{K} \underline{\Delta r}. \quad (4-8)$$

The necessary condition for the functional  $V^*$  to assume a stationary value

$$\delta V^* = 0, \quad (4-9)$$

gives the incremental equilibrium equations

$$\underline{K} \underline{\Delta r} = \underline{\Delta R}, \quad (4-10)$$

for the unknown displacement vector  $\underline{\Delta r}$ . Eq.(4-10) will be solved in section IV.

### III. Constitutive Equations:-Elasto-plastic Matrix

The elasto-plastic matrix based upon the Prandtl-Reuss theory and the Von Mises yield criterion was first presented by Y. Yamada (14). A few years later O.C. Zienkiewicz (15) and his colleagues presented a matrix of the same form which was good for any yield criterion. The basic part of Zienkiewicz's development is presented here for completeness and the matrix on which the current program was based is also developed.

Rewrite equations (2-30), (2-31), and (2-43) in matrix form

$$d[\varepsilon] = d[\varepsilon]_e + d[\varepsilon]_p, \quad (4-11)$$

$$d[\varepsilon]_e = [D]^{-1} d[\sigma], \quad (4-12)$$

$$d[\varepsilon]_p = d\lambda \frac{\partial f}{\partial [\sigma]}, \quad (4-13)$$

and thus

$$d[\varepsilon] = [D]^{-1} d[\sigma] + \frac{\partial f}{\partial [\sigma]} d\lambda, \quad (4-14)$$

where

$$[D] = 2G \begin{bmatrix} p & q & q & 0 & 0 & 0 \\ q & p & q & 0 & 0 & 0 \\ q & q & p & 0 & 0 & 0 \\ 0 & 0 & 0 & \frac{1}{2} & 0 & 0 \\ 0 & 0 & 0 & 0 & \frac{1}{2} & 0 \\ 0 & 0 & 0 & 0 & 0 & \frac{1}{2} \end{bmatrix}, \quad (4-15)$$

In which

$$p = \frac{1-\nu}{1-2\nu}; \quad q = \frac{\nu}{1-2\nu}.$$

When plastic flow is occurring the stresses are on the yield surface,  $f = 0$  and  $df = 0$ . Thus, from Eq.(2-29),

$$\frac{\partial f}{\partial \sigma_{ij}} d\sigma_{ij} + \frac{\partial f}{\partial \varepsilon_{ij}^p} d\varepsilon_{ij}^p + \frac{\partial f}{\partial \kappa} d\kappa = 0,$$

or

$$\left[ \frac{\partial f}{\partial [\sigma]} \right]^T d[\sigma] - A d\lambda = 0, \quad (4-16)$$

where

$$A = - \left( \frac{\partial f}{\partial \varepsilon_{ij}^p} d\varepsilon_{ij}^p + \frac{\partial f}{\partial \kappa} d\kappa \right) \frac{1}{d\lambda}. \quad (4-17)$$

Multi. Eq.(4-14) by  $\left[ \frac{\partial f}{\partial [\sigma]} \right]^T [D]$ , leads to

$$\left[ \frac{\partial f}{\partial [\sigma]} \right]^T [D] d[\varepsilon] = \left[ \frac{\partial f}{\partial [\sigma]} \right]^T d[\sigma] + \left[ \frac{\partial f}{\partial [\sigma]} \right]^T [D] \left[ \frac{\partial f}{\partial [\sigma]} \right] d\lambda \quad (4-18)$$

Sub. Eq.(4-16) into Eq.(4-18), yields

$$\left[ \frac{\partial f}{\partial [\sigma]} \right]^T [D] d[\varepsilon] = A d\lambda + \left[ \frac{\partial f}{\partial [\sigma]} \right]^T [D] \left[ \frac{\partial f}{\partial [\sigma]} \right] d\lambda$$

$$d\lambda = \frac{\left[ \frac{\partial f}{\partial [\sigma]} \right]^T [D] d[\varepsilon]}{A + \left[ \frac{\partial f}{\partial [\sigma]} \right]^T [D] \left[ \frac{\partial f}{\partial [\sigma]} \right]} \quad (4-19)$$

Sub. Eq.(4-19) into Eq.(4-14), leads to

$$d[\varepsilon] = [D]^{-1} d[\sigma] + \frac{\left[ \frac{\partial f}{\partial [\sigma]} \right] \left[ \frac{\partial f}{\partial [\sigma]} \right]^T [D] d[\varepsilon]}{A + \left[ \frac{\partial f}{\partial [\sigma]} \right]^T [D] \left[ \frac{\partial f}{\partial [\sigma]} \right]}$$

$$d[\sigma] = [D] d[\varepsilon] - \frac{[D] \left[ \frac{\partial f}{\partial [\sigma]} \right] \left[ \frac{\partial f}{\partial [\sigma]} \right]^T [D]}{A + \left[ \frac{\partial f}{\partial [\sigma]} \right]^T [D] \left[ \frac{\partial f}{\partial [\sigma]} \right]} \cdot d[\varepsilon]$$

or 
$$d[\sigma] = [D]_{ep}^* d[\varepsilon], \quad (4-20)$$

where 
$$[D]_{ep}^* = [D] - \frac{[D] \left[ \frac{\partial f}{\partial [\sigma]} \right] \left[ \frac{\partial f}{\partial [\sigma]} \right]^T [D]}{A + \left[ \frac{\partial f}{\partial [\sigma]} \right]^T [D] \left[ \frac{\partial f}{\partial [\sigma]} \right]}. \quad (4-21)$$

Thus in plastic flow analysis, the elasto-plastic matrix  $[D]_{ep}^*$  replaces the elastic matrix  $[D]$ .  $[D]_{ep}^*$  may be interpreted physically as the required correction to the elastic stress-strain relation which keeps the stress increment on the expanding yield surface (or tangential to the yield surface in the case of elastic-perfectly plastic materials). It is symmetric, positive definite and is valid whether  $A$  is zero or not.

For isotropic plasticity, it is reasonable to assume that (33)

$$\frac{\partial f}{\partial \varepsilon_{ij}^p} \equiv 0.$$

Thus, Eq.(4-17) becomes

$$A = - \frac{\partial f}{\partial K} dK \frac{1}{d\lambda}. \quad (4-22)$$

For isotropic perfect plasticity, where  $K = \text{constant}$ ,  $dK = 0$ ,

$$\therefore A \equiv 0.$$

For isotropic work-hardening plasticity, the plastic work done is defined by

$$dK = dW_p = S_{ij} d\varepsilon_{ij}^p,$$

but

$$d\varepsilon_{ij}^p = \frac{\partial f}{\partial \sigma_{ij}} d\lambda,$$

and

$$\therefore dK = S_{ij} \frac{\partial f}{\partial \sigma_{ij}} d\lambda,$$

$$A = - \frac{\partial f}{\partial K} S_{ij} \frac{\partial f}{\partial \sigma_{ij}}.$$

If the Von Mises yield criterion

$$f = \frac{1}{2} \left[ S_x^2 + S_y^2 + S_z^2 + 2(S_{xy}^2 + S_{yz}^2 + S_{zx}^2) \right]$$

is employed. Then

$$dK = \bar{\sigma} d\bar{\varepsilon}^p,$$

$$\frac{\partial f}{\partial K} = - \frac{d\bar{\sigma}}{dK} = - \frac{d\bar{\sigma}}{d\bar{\varepsilon}^p} \cdot \frac{1}{\bar{\sigma}} = - \frac{H'}{\bar{\sigma}},$$

$$\frac{\partial f}{\partial \sigma_{ij}} = \frac{3}{2} \cdot \frac{S_{ij}}{\bar{\sigma}},$$

and

$$A = \frac{H'}{\bar{\sigma}^2} \cdot \frac{3}{2} S_{ij} S_{ij},$$

noting that

$$S_{ij} S_{ij} = \frac{2}{3} \bar{\sigma}^2,$$

$$\therefore A = H'. \quad (4-23)$$

Where  $\bar{\sigma}$ ,  $d\bar{\varepsilon}^p$ , and  $H'$  are defined in chapter two.





and the denominator

$$A + \left[ \frac{\partial f}{\partial [\sigma]} \right]^T [D] \left[ \frac{\partial f}{\partial [\sigma]} \right] = H' + \frac{3}{2\bar{\sigma}} \begin{bmatrix} S_x & S_y & S_z & 2S_{xy} & 2S_{yz} & 2S_{zx} \end{bmatrix} \frac{3G}{\bar{\sigma}} \begin{bmatrix} S_x \\ S_y \\ S_z \\ S_{xy} \\ S_{yz} \\ S_{zx} \end{bmatrix}$$

$$= \frac{9G}{2\bar{\sigma}^2} \left[ S_x^2 + S_y^2 + S_z^2 + 2S_{xy}^2 + 2S_{yz}^2 + 2S_{zx}^2 \right] + H'$$

$$= 3G + H'$$

Thus Eq.(4-21) can be written as

$$[D]_{ep}^* = [D] - \frac{3G}{\bar{\sigma}^2 \left( 1 + \frac{H'}{3G} \right)} \begin{bmatrix} S_x & & & & & & \\ S_x S_y & S_y^2 & & & & & \\ S_x S_z & S_y S_z & S_z^2 & & & & \\ S_x S_{xy} & S_y S_{xy} & S_z S_{xy} & S_{xy}^2 & & & \\ S_x S_{yz} & S_y S_{yz} & S_z S_{yz} & S_{xy} S_{yz} & S_{yz}^2 & & \\ S_x S_{zx} & S_y S_{zx} & S_z S_{zx} & S_{xy} S_{zx} & S_{yz} S_{zx} & S_{zx}^2 & \end{bmatrix} \text{ SYMM}$$

For two dimensional plane stress problems, the elastoplastic matrix becomes

$$[D]_{ep}^* = \frac{E}{R} \begin{bmatrix} S_y^2 + 2Z & & & \text{SYMM} \\ -S_x S_y + 2\nu Z & S_x^2 + 2Z & & \\ -\frac{S_x + \nu S_y}{1 + \nu} S_{xy} & -\frac{S_y + \nu S_x}{1 + \nu} S_{xy} & \frac{R - 2(1 - \nu) S_{xy}^2}{2(1 + \nu)} & \end{bmatrix} \quad (4-24)$$

where

$$Z = \frac{S_{xy}^2}{1 + \nu} + \frac{2H'\bar{\sigma}^2}{9E},$$

$$R = 2(1 - \nu^2)Z + S_x^2 + 2\nu S_x S_y + S_y^2.$$

#### IV. Solution of Plasticity Equations

The global stiffness matrix in Eq.(4-5) is different from the linear elastic case, since for elasto-plastic problems the matrix  $[D]_{ep}^*$  is itself a function of current state of stress. The incremental equilibrium equation, Eq.(4-10), is therefore nonlinear and cannot be solved by a simple matrix inversion. Two well-known methods, Newton-Raphson and modified Newton-Raphson, are used to solve the nonlinear incremental equilibrium equations. The procedures are now briefly outlined.

##### a. Newton-Raphson Method

Consider a system of nonlinear equations, for example,

$$[\Delta R] = [F([\Delta r])] \quad \text{Eq.(4-25)}$$

we may write

$$[g([\Delta r])] = [\Delta R] - [F([\Delta r])]$$

where  $[\Delta r]$  is the variable and  $[\Delta R]$  is a known load increment.

At the "correct" value of  $[\Delta r]$  - the value which solves Eq.(4-25) -

we have

$$[g([\Delta r])] = 0 \quad \text{Eq.(4-26)}$$

Let us expand  $[g]$  as a Taylor series about some test value  $[\Delta r]_0$ , such that

$$[\Delta r] = [\Delta r]_0 + [\delta r]$$

Then

$$[g([\Delta r])] = [g([\Delta r]_0)] + \left. \frac{\partial [g]}{\partial [\Delta r]} \right|_{\Delta r = \Delta r_0} [\delta r] + \text{h.o.t. in } \delta r$$

$$= [0]$$

by Eq.(4-26)

But

$$\left. \frac{\partial [g]}{\partial [\Delta r]} \right|_{\Delta r_0} = - \left. \frac{\partial [F]}{\partial [\Delta r]} \right|_{\Delta r_0}$$

from Eq.(4-25)

$$= - [k]_0$$

(4-27)

where  $[k]$  is the "tangential stiffness matrix" as defined by Eq.(4-10). Thus

$$\begin{aligned} [g]_0 &= [k]_0 [\delta r] \\ &= [k]_0 [\Delta r] - [k]_0 [\Delta r]_0 \end{aligned}$$

Now  $[k]$  is the Jacobian matrix of the function  $[F]$  and is therefore invertable, so

$$[\Delta r]_1 = [\Delta r]_0 - [k]_0^{-1} [g]_0 \quad (4-28)$$

These arguments are illustrated diagrammatically in Fig.4-3.

This value of  $[\Delta r]_1$  is, of course, only approximate, but it can be used as a starting value for another step in the iterative process. The algorithm is simply;

$$[\Delta r]_{m+1} = [\Delta r]_m - [k]_m^{-1} [g]_m \quad (4-29)$$

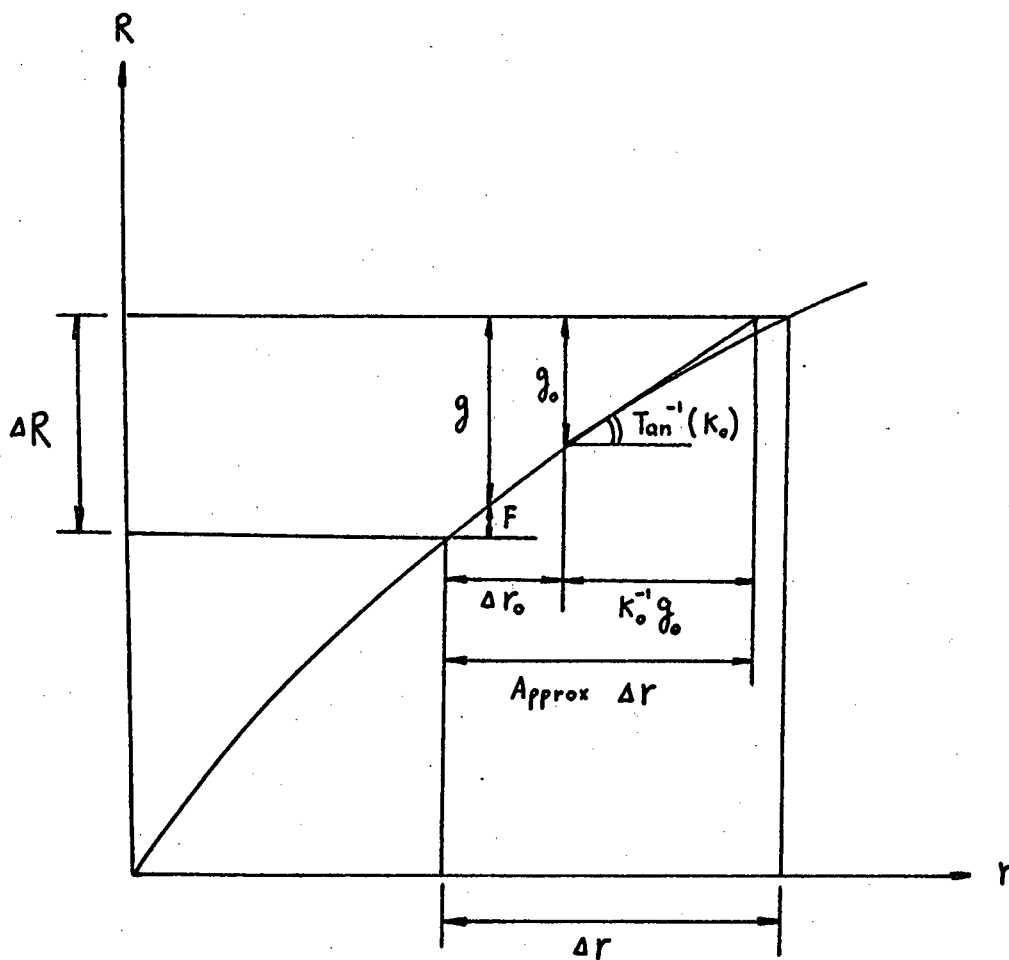


FIG.4-3 THE ILLUSTRATIONS OF EQS.(4-25), (4-26), (4-27) AND (4-28)

This process is repeated until the residual force  $[q]_m$  or the increments of displacements  $([\Delta r]_{m+1} - [\Delta r]_m)$  become zero, or within a prescribed criterion.

b. Modified Newton-Raphson Method

The Newton-Raphson method could indeed be used, but it is generally inconvenient since the tangential stiffness matrix depends on the current stress levels and has to be calculated at each step of the iterative process. Moreover, we have to invert a very large matrix everytime. This difficulty, however, can be overcome by an alternative process of iteration, known as the modified Newton-Raphson method, in which only the initial stiffness matrix is used. Then, instead of Eq.(4-29), we have

$$[\Delta r]_{m+1} = [\Delta r]_m - [k]_0^{-1} [q]_m. \quad (4-30)$$

These two methods are shown diagrammatically (for one variable) in Figs.4-4a and 4-4b. In fact, it is generally found to be adequate to compute  $[k]_0^{-1}$  for the first load increment-the elastic case- and to use this value for all subsequent load increments.

Obviously, the number of iterations required for convergence in the modified method is greater than in the standard method; however, the actual calculation and amount of computing time required is, in fact, less than that for the standard Newton-Raphson method because it is not necessary to invert a new stiffness matrix at each cycle. In the present study, the modified Newton-Raphson iterative method is preferred.

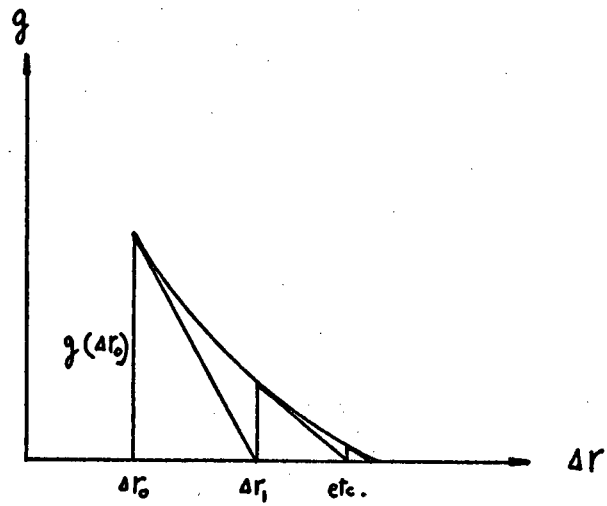


FIG.4-4a NEWTON-RAPHSON METHOD

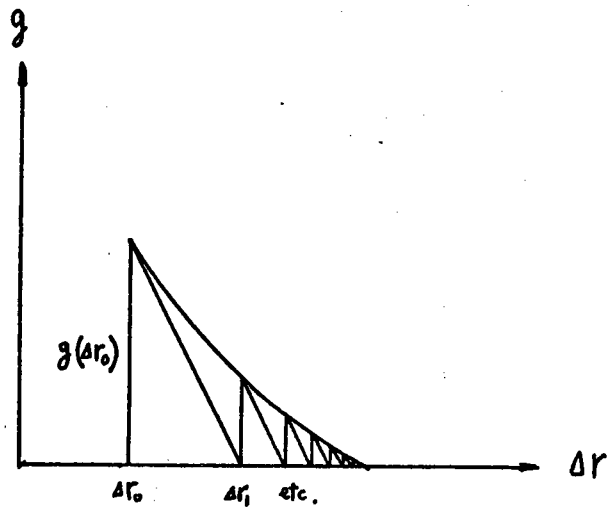


FIG.4-4b MODIFIED NEWTON-RAPHSON METHOD



## V. Calculation Procedure

It has been mentioned that a combination of the method of incremental loading and the modified Newton-Raphson method generates the complete nonlinear response by a sequence of piece-wise linear steps. Thus the total load vector  $[R]$  to be applied to the system is divided into suitable small increments  $[\Delta R]^n$  and an available computer program developed for the linear elastic problem has been adjusted to the elastoplastic problem by minor modifications.

Since the inverse of the tangential stiffness matrix  $[K_o]^{-1}$  is used throughout the process, it is computed at the very beginning for convenience.  $[K_o]$  depends on the elastic constants and the structural geometry only. The following indices are used:

$n$  = number of load increment

$m$  = number of iteration

### a. Procedure:

A. Starting with a trial solution for the  $n^{\text{th}}$  increment

$$\Delta [r]_o^n = [0]_o,$$

and the load increment  $[\Delta R]^n$ , compute the residual force

$$[g]_o^n = -[\Delta R]^n.$$

B. Iterative loops:

1. Compute the approximate solution

$$[\Delta r]_{m+1}^n = [\Delta r]_m^n - [K]_0^{-1} [q]_m^n,$$

$$(m = 0, 1, 2, 3, \dots)$$

2. compute the elastic increment of strain  $\Delta \underline{\xi}_{m+1}^{ne}$  and stress  $\Delta \underline{\sigma}_{m+1}^{ne}$  corresponding to  $[\Delta r]_{m+1}^n$  i.e.

$$\Delta \underline{\xi}_{m+1}^{ne} = \underline{L} \underline{A} \underline{a} [\Delta r]_{m+1}^n,$$

$$\Delta \underline{\sigma}_{m+1}^{ne} = \underline{D} \Delta \underline{\xi}_{m+1}^{ne}.$$

3. add  $\Delta \underline{\sigma}_{m+1}^{ne}$  to the current stress existing at the start of the iteration  $\underline{\sigma}_m^n$  to obtain

$$\underline{\sigma}_{m+1}^{ne} = \underline{\sigma}_m^n + \Delta \underline{\sigma}_{m+1}^{ne}.$$

4. if  $f(\underline{\sigma}_{m+1}^{ne}, \kappa) < 0$  only elastic strains occur, and the state variables for the start of the next load increment are

$$\underline{\sigma}_0^{n+1} = \underline{\sigma}_{m+1}^n,$$

$$\underline{\xi}_0^{n+1} = \underline{\xi}_m^n + \Delta \underline{\xi}_{m+1}^{ne}.$$

Go to A and start the next load increment.

5. if  $f(\underline{\sigma}_{m+1}^{ne}, \kappa) \geq 0$  and  $f(\underline{\sigma}_m^n, \kappa) \equiv 0$  then

- (i) compute the actual stress  $\Delta \underline{\sigma}_{m+1}^{na}$  due to the nonlinear stress-strain relation using the elasto-plastic matrix, i.e.

$$\Delta \underline{\sigma}_{m+1}^{na} = \underline{D}_{ep}^* \Delta \underline{\xi}_{m+1}^{ne},$$

where

$$\underline{D}_{ep}^* = \underline{D}_{ep}^* (\underline{\sigma}_{m+1}^{ne}).$$

(ii) compute the residual stress

$$\Delta \underline{\sigma}_{m+1}^{nr} = \Delta \underline{\sigma}_{m+1}^{ne} - \Delta \underline{\sigma}_{m+1}^{na}.$$

6. if  $f(\underline{\sigma}_{m+1}^{ne}, \kappa) \geq 0$  and  $f(\underline{\sigma}_m^n, \kappa) < 0$  then increase the value of  $\underline{\sigma}_m^n$  to  $\underline{\sigma}_m^{n*}$  by interpolation such that  $f(\underline{\sigma}_m^{n*}, \kappa) \equiv 0$  then compute

$$\Delta \underline{\sigma}_{m+1}^{ne*} = \underline{\sigma}_{m+1}^{ne} - \underline{\sigma}_m^{n*},$$

$$\Delta \underline{\varepsilon}_{m+1}^{ne*} = \underline{D}^{-1} \Delta \underline{\sigma}_{m+1}^{ne*},$$

$$\Delta \underline{\sigma}_{m+1}^{na} = \underline{D}_{ep}^* \Delta \underline{\varepsilon}_{m+1}^{ne*},$$

and

$$\Delta \underline{\sigma}_{m+1}^{nr} = \Delta \underline{\sigma}_{m+1}^{ne*} - \Delta \underline{\sigma}_{m+1}^{na}.$$

7. compute the current stress and strain

$$\underline{\sigma}_{m+1}^n = \underline{\sigma}_{m+1}^{ne} - \Delta \underline{\sigma}_{m+1}^{nr},$$

$$\underline{\varepsilon}_{m+1}^n = \underline{\varepsilon}_m^n + \Delta \underline{\varepsilon}_{m+1}^{ne}.$$

8. compute the residual force (see section b)

$$[g]_{m+1}^n = \int_V (\underline{L} \underline{A} \underline{a})^T \Delta \underline{\sigma}_{m+1}^{ni} dV,$$

and the new  $\kappa$ . In the current work, a constant strain element is used,  $\Delta \underline{\sigma}_{m+1}^{ni}$  is constant, and the intergration is linear.

9. if  $\| [g]_{m+1}^n \| \ll \| [g]_0^n \|$  i.e. if some selected criterion for the smallness of  $[g]_{m+1}^n$  is satisfied, then let

$$\underline{\sigma}_0^{n+1} = \underline{\sigma}_{m+1}^n,$$

and go to A to start the next load increment. Otherwise, go to B and begin the next iteration.

b. Residual Force Vector

(i) Consider a typical triangular element (Fig.4-5),

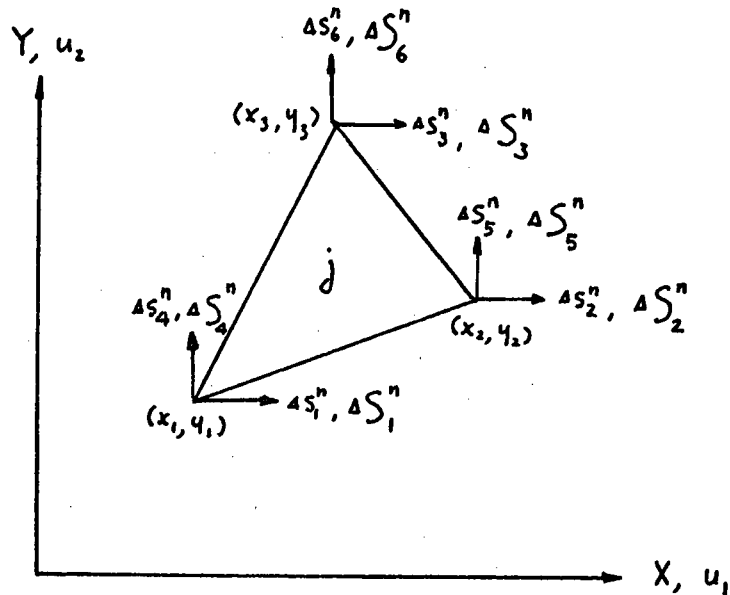


FIG.4-5 CONSTANT STRAIN ELEMENT

and write the principle of virtual work equation:

$$\delta (\underline{\Delta S}^n)^T \underline{\Delta S}^n = \int_{V_j} \delta (\underline{\Delta \underline{\epsilon}}^n)^T \underline{\Delta \underline{\sigma}}^n dV,$$

but

$$\underline{\Delta \underline{\epsilon}}^n = \underline{L} \underline{A} \underline{\Delta S}^n,$$

$$\therefore \delta (\underline{\Delta S}^n)^T \underline{\Delta S}^n = \delta (\underline{\Delta S}^n)^T \int_{V_j} (\underline{L} \underline{A})^T \underline{\Delta \underline{\sigma}}^n dV.$$

For arbitrary  $\delta(\Delta \underline{S}^n)$  we have

$$\Delta \underline{S}^n = \int_{V_j} (\underline{L} \underline{A})^T \Delta \underline{\sigma}^n dV .$$

Since  $\Delta \underline{\sigma}^n$  is the actual stress due to  $[\Delta R]^n$ , we can write the above equation as

$$\Delta \underline{S}^n = \int_{V_j} (\underline{L} \underline{A})^T \Delta \underline{\sigma}_{m+1}^{na} dV .$$

(ii) The residual force vector is given by

$$\begin{aligned} [g]_{m+1}^n &= \sum_j \int_{V_j} (\underline{L} \underline{A} \underline{a})^T \Delta \underline{\sigma}_{m+1}^{ne} dV - \sum_j \underline{a}^T \Delta \underline{S}^n \\ &= \sum_j \int_{V_j} (\underline{L} \underline{A} \underline{a})^T (\Delta \underline{\sigma}_{m+1}^{ne} - \Delta \underline{\sigma}_{m+1}^{na}) dV . \end{aligned}$$

Noting that

$$\Delta \underline{\sigma}_{m+1}^{nr} = \Delta \underline{\sigma}_{m+1}^{ne} - \Delta \underline{\sigma}_{m+1}^{na} ,$$

$$\therefore [g]_{m+1}^n = \sum_j \int_{V_j} (\underline{L} \underline{A} \underline{a})^T \Delta \underline{\sigma}_{m+1}^{nr} dV ,$$

$$\text{or } [g]_{m+1}^n = \int_V (\underline{L} \underline{A} \underline{a})^T \Delta \underline{\sigma}_{m+1}^{nr} dV ,$$

where we have implied the integration over the whole volume.

#### IV. Example of Numerical Results

##### a. Perforated Strip: Strain Hardening Material

The problem of determining the elastic-plastic strain and stress distribution that occurs in thin perforated strips of a strain hardening material when the applied stress is increased monotonically from the elastic region of loading to values producing an impending plastic flow, was investigated by Theocaris and Marketos. In (34) they report results of an experimental strain analysis. Using photoelastic coating and electrical analogy techniques total strains were determined. Stresses were estimated by applying the Prandtl-Reuss incremental plasticity relations Eq. (2-42). In this fashion a measure of the elastic strains and, hence of the plastic strains, could be obtained by Eq.(2-30).

The finite element idealization of the geometry under consideration is shown in Fig. 4-6. The idealized uniaxial stress-strain diagram of the strip material, aluminum alloy 57S, is reproduced in Fig. 4-7. In Fig. 4-8 the development of maximum strain in the longitudinal direction as obtained from finite element results is shown, together with similar results published by Theocaris and Marketos, for different values of the applied load. In Fig. 4-9, a comparison can be made

between the development of plastic zones as reported in (34) and as computed by finite elements. The load factor  $\lambda$  is defined as

$$\lambda = \frac{\text{Applied load}}{\text{Load at which yield begins by closed form solution}}$$

Finally, Fig. 4-10 shows the equivalent stress v.s. strain, equations (2-34) and (2-35), in the element which yielded first. The curve shows that the finite element solution is following the hardening rule specified.

b. Perforated Plate: Elastic-perfectly-plastic Material

The problem solved in (a) was repeated, but with elastic-perfectly-plastic material, ie.  $H'=0$ , Eq. (2-39). In order to compare the result with the strain hardening case, the development of the maximum strain in the longitudinal direction is shown in Fig. 4-8. It is interesting to note that there is only a little difference at higher loads.

c. Deep Cantilever Beam:

The dimensions and loading conditions are shown in Fig. 4-11, in which the finite element net is presented.



The material used is shown in Fig. 4-12. In Fig. 4-13 the ratio  $\lambda$  is defined and the development of the plastic zones for different values of  $\lambda$  is shown. The region enclosed by the dashed line was not calculated by the program, because when the highest load was applied ( $\lambda = 1$ ), no convergence could be obtained. This problem was solved in reference (35) and a similar experience was noted. Figs. 4-14 and 4-15 show the distribution of normal and shear stress acting across the sections AA' and BB' respectively.

d. Right-angle Notch: Elastic-perfectly-plastic Material

The Right-angle Notch with a notch to half-width ratio of 1 to 2 is shown in Fig. 4-15, wherein the finite element net is presented. An elastic-perfectly-plastic material was assumed: uniaxial yield stress  $\sigma_0 = 24.3 \text{ Kg/mm}^2$   
 $E = 7000 \text{ Kg/mm}^2$ ,  $H' = 0$ ,  $\nu = 0.2$ .

The development of the maximum strain in the longitudinal direction for loading is shown in Fig. 4-17, wherein the curve for a circular notch is also shown for comparison. Fig. 4-18a shows the development of the plastic enclaves obtained by D. Allen and R. Southwell (36). They assumed that there is no volume change in either elastic or plastic deformation and solved the stress function by a relaxation method. Fig. 4-18b shows the finite element results for different loading paths. These two plastic zones are of the same general shape.

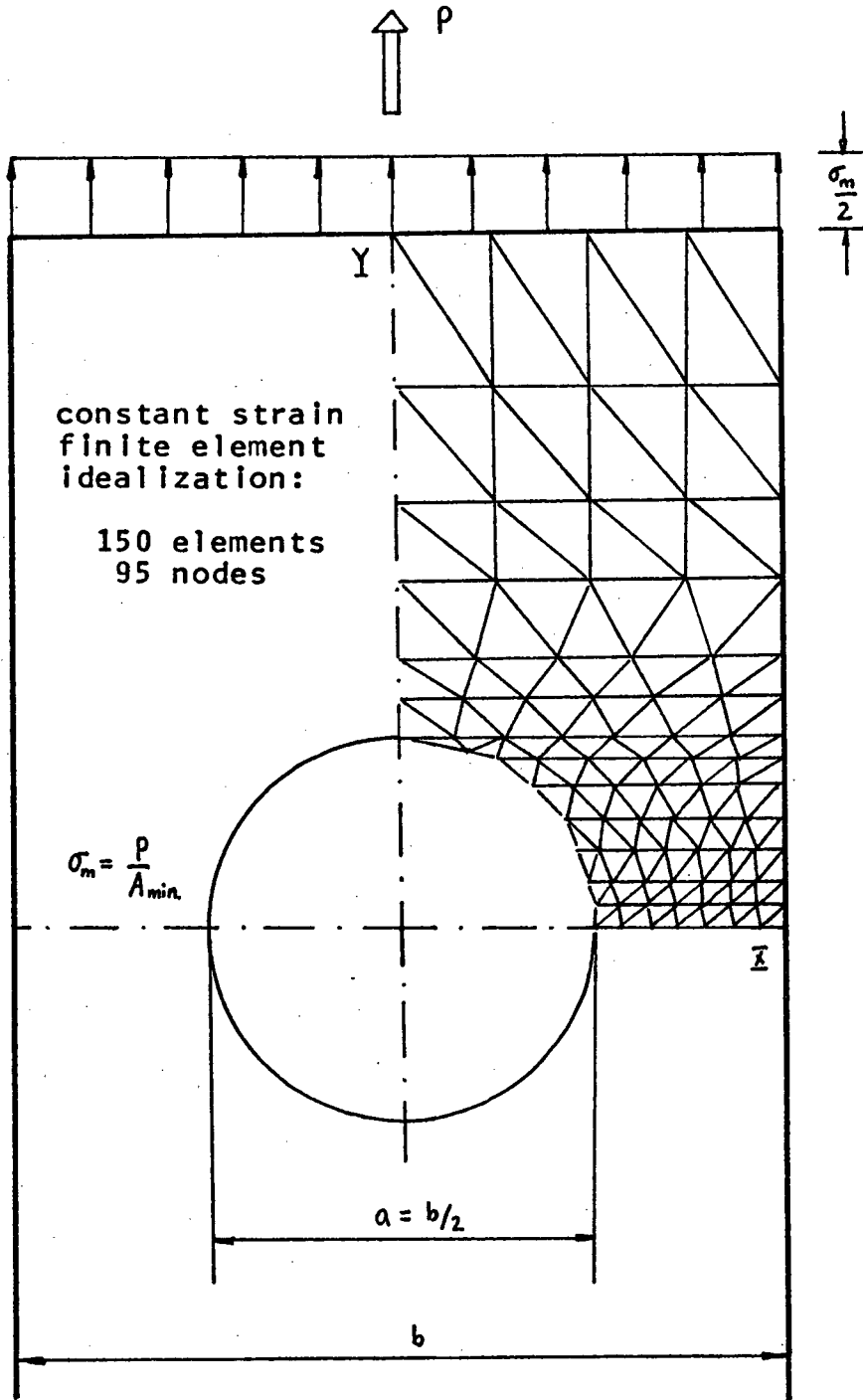
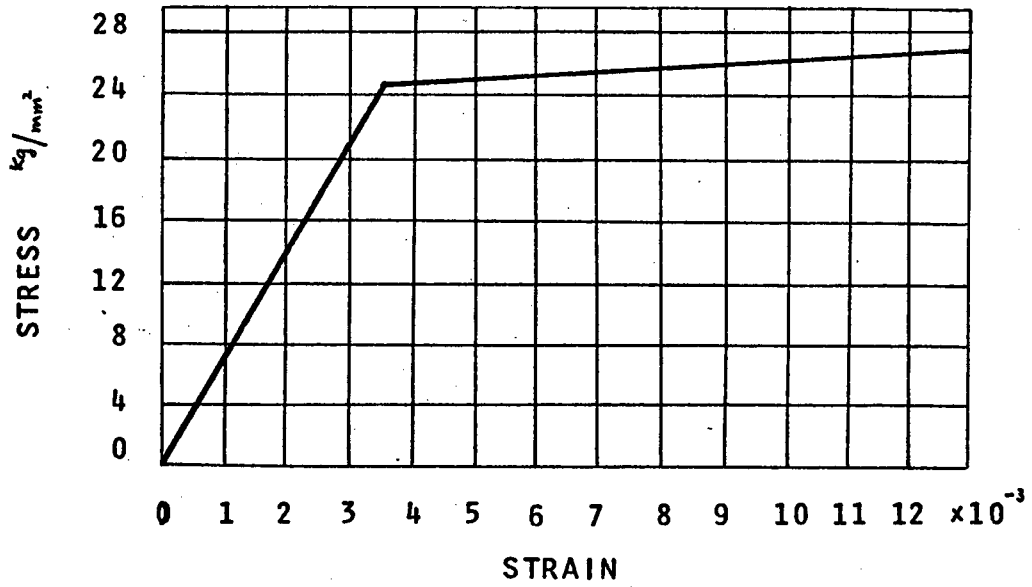
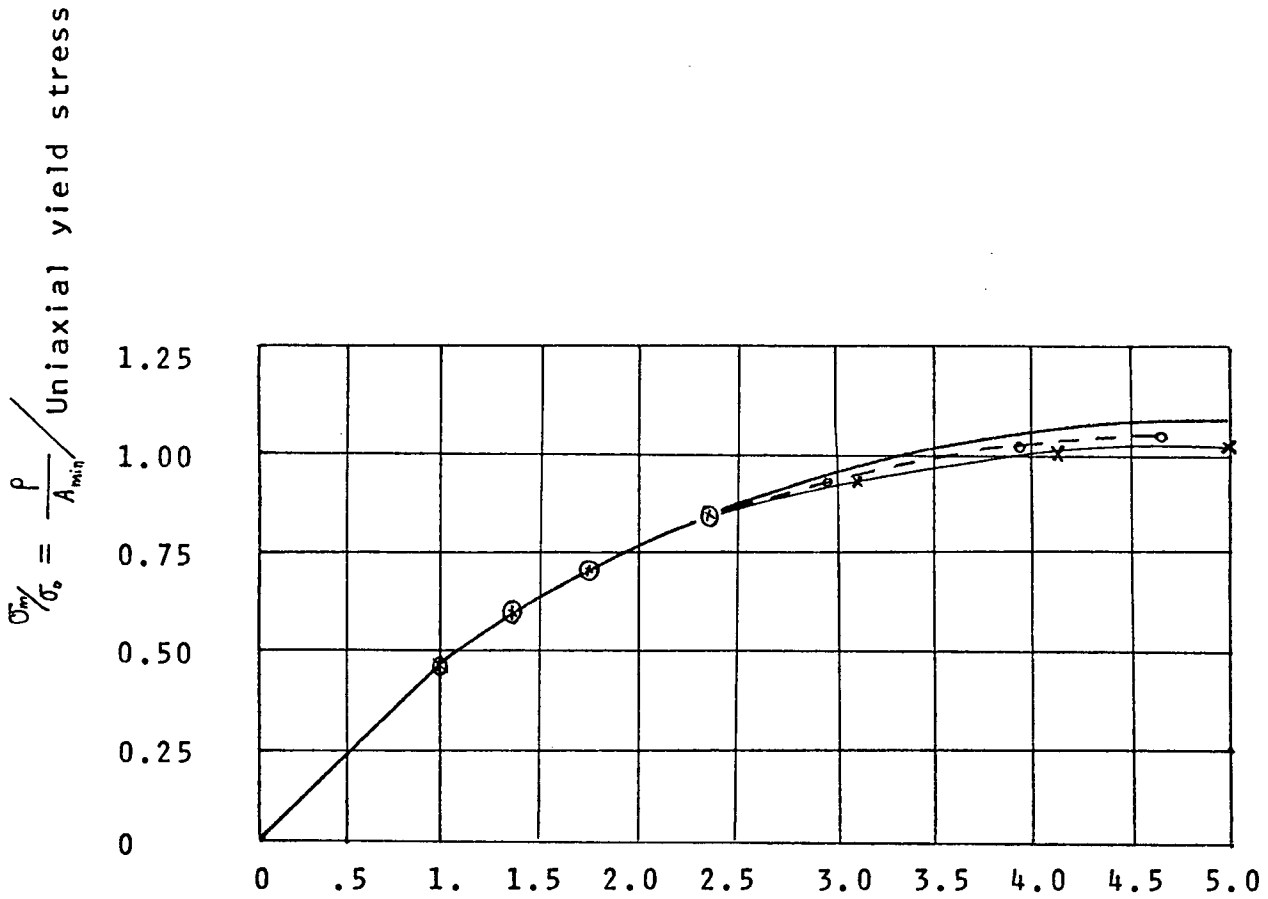


FIG.4-6 UNIFORMLY LOADED PERFORATED STRIP



yield stress in pure tension  $\sigma_0 = 24.3 \text{ kg/mm}^2$   
slope of work-hardening curve  $H = 225.0 \text{ kg/mm}^2$   
modulus of elasticity  $E = 7000.0 \text{ kg/mm}^2$

FIG.4-7 UNIAXIAL STRESS-STRAIN CURVE



MAX. STRAIN IN THE LONGITUDINAL DIRECTION  $\frac{E\epsilon}{\sigma_0}$

- experimental from Theocaris & Marketos
  - finite element solution
  - ×---× finite element solution for elastic perfectly plastic material
- } work hardening

FIG.4-8 END LOAD vs. MAX STRAIN FOR PERFORATED STRIP

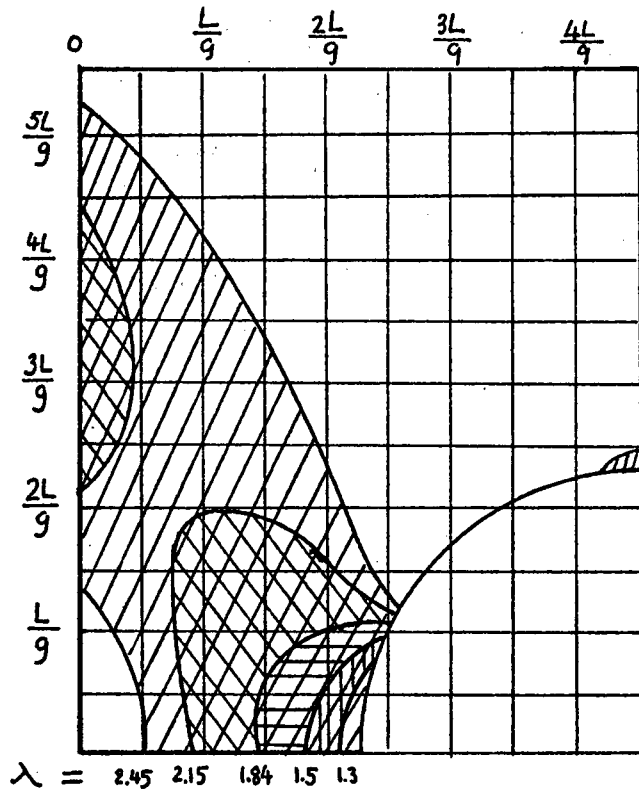


FIG. 4-9a  
EXPERIMENTAL RESULTS

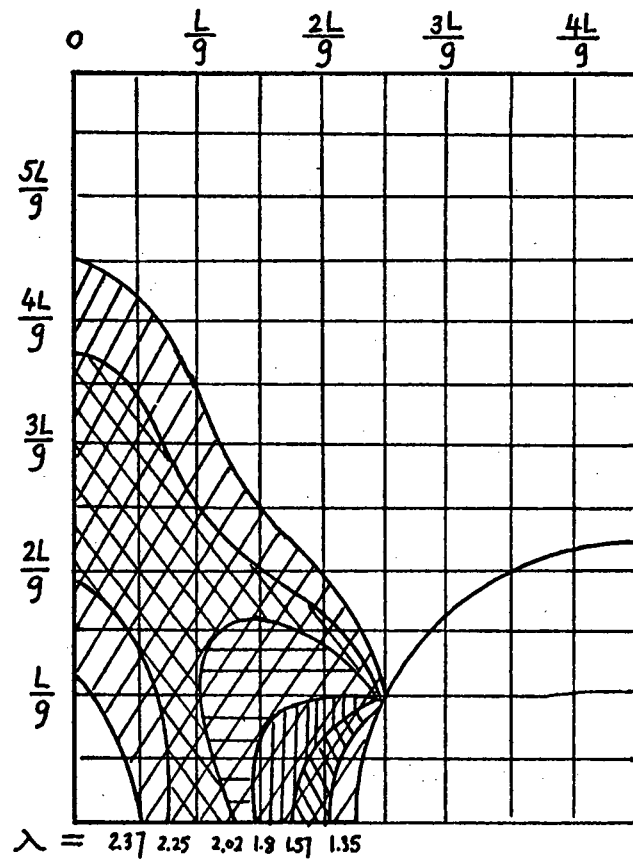
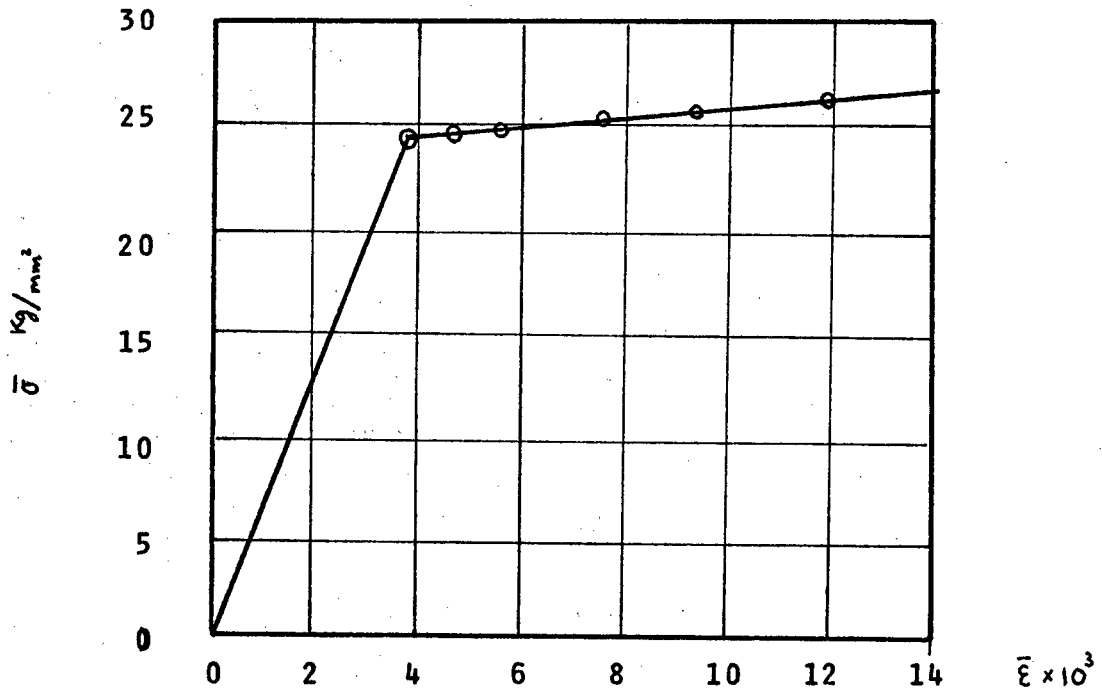


FIG. 4-9b  
FINITE ELEMENT RESULTS

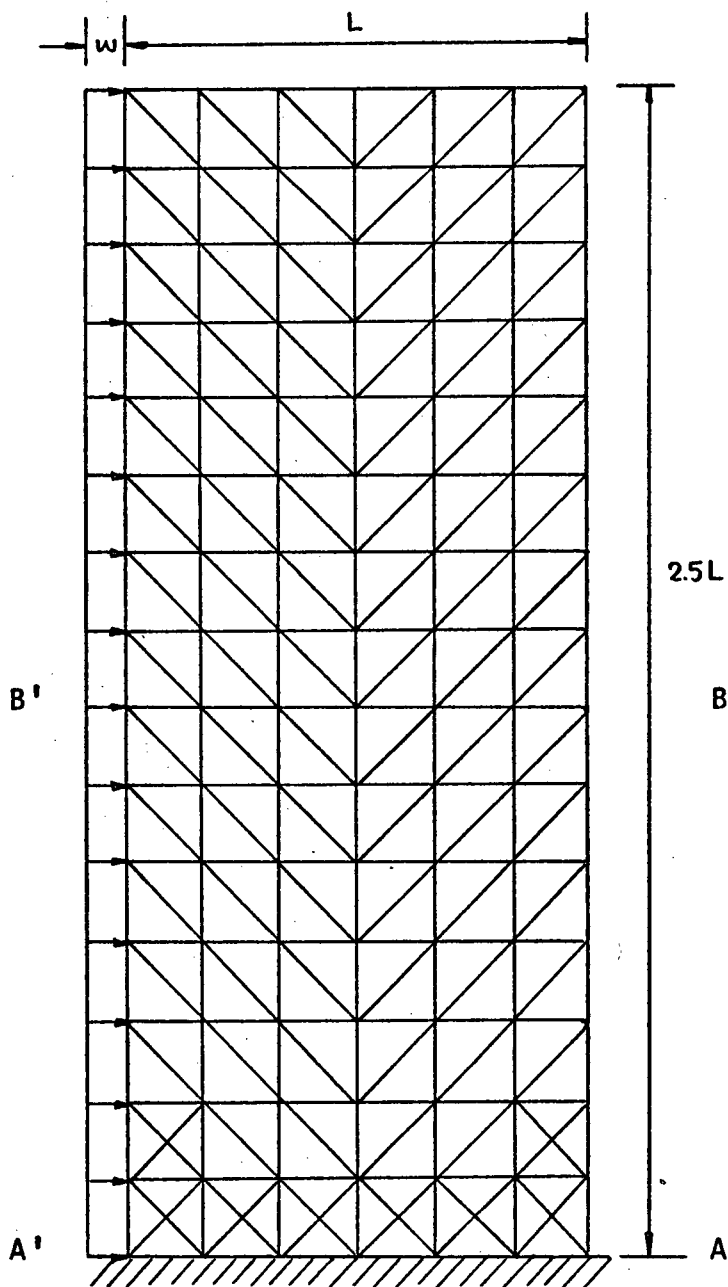


$$\bar{\sigma} = \sqrt{\frac{3}{2} S_{ij} S_{ij}}$$

$$d\bar{\epsilon}^p = \sqrt{\frac{2}{3} d\epsilon_{ij}^p d\epsilon_{ij}^p}$$

$$\bar{\epsilon} = \frac{\sigma_0}{E} + \int d\bar{\epsilon}^p$$

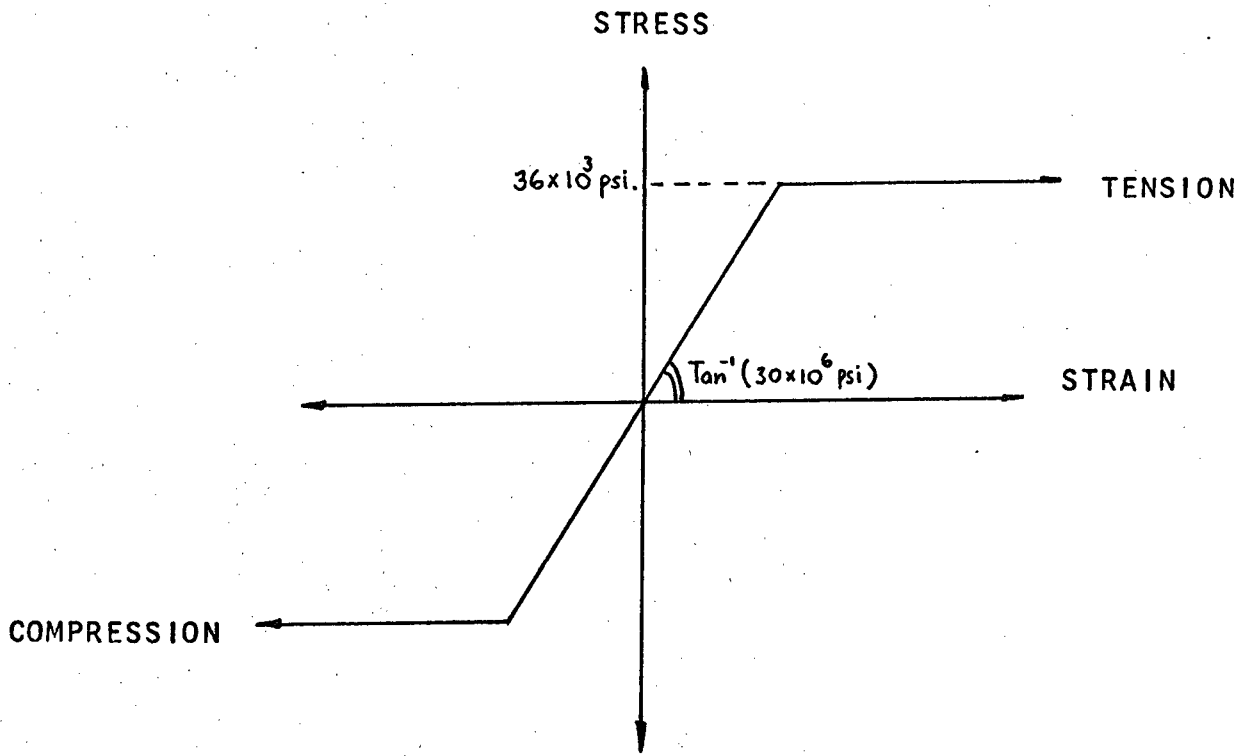
FIG.4-10 EQUIVALENT STRESS vs. EQUIVALENT STRAIN IN THE ELEMENT WHICH YIELD FIRST



Finite Element Idealization:

196 elements  
120 nodes

FIG.4-11 SHEAR WALL SUBJECTED TO LATERAL LOAD



yield stress =  $36 \times 10^3$  psi.  
modulus of elasticity =  $30 \times 10^6$  psi.

FIG.4-12 UNIAXIAL STRESS-STRAIN CURVE



$$\lambda = \frac{\text{APPLIED LOAD}}{\text{LIMIT LOAD COMPUTED FROM PLASTIC BEAM THEORY}}$$

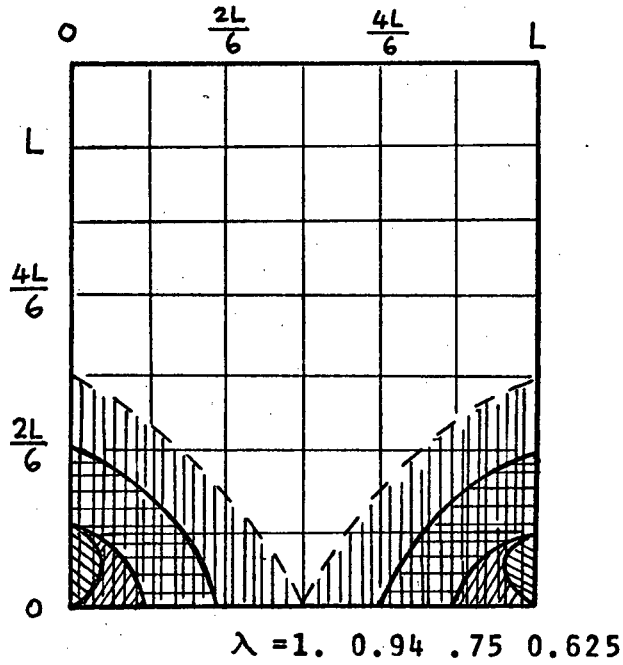


FIG.4-13 DEVELOPMENT OF PLASTIC ZONES FOR DIFFERENT VALUES OF  $\lambda$

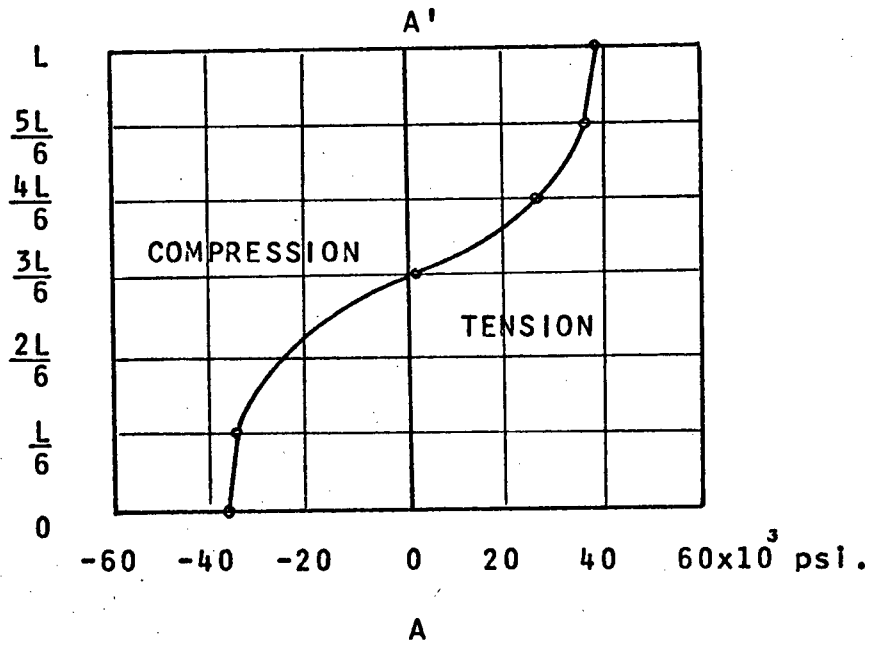


FIG.4-14a NORMAL STRESS DISTRIBUTION AT HIGHEST LOAD

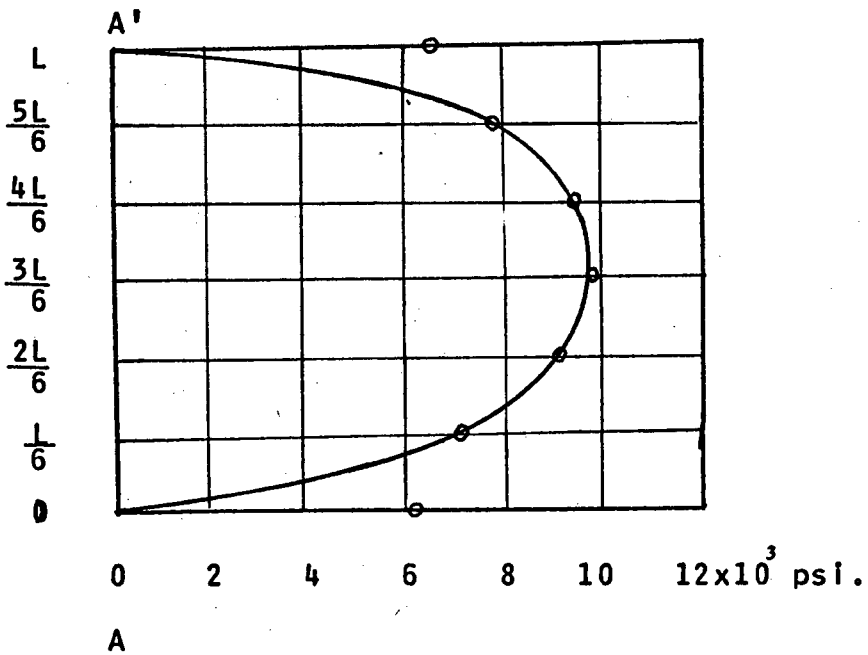


FIG.4-14b SHEAR STRESS DISTRIBUTION AT HIGHEST LOAD

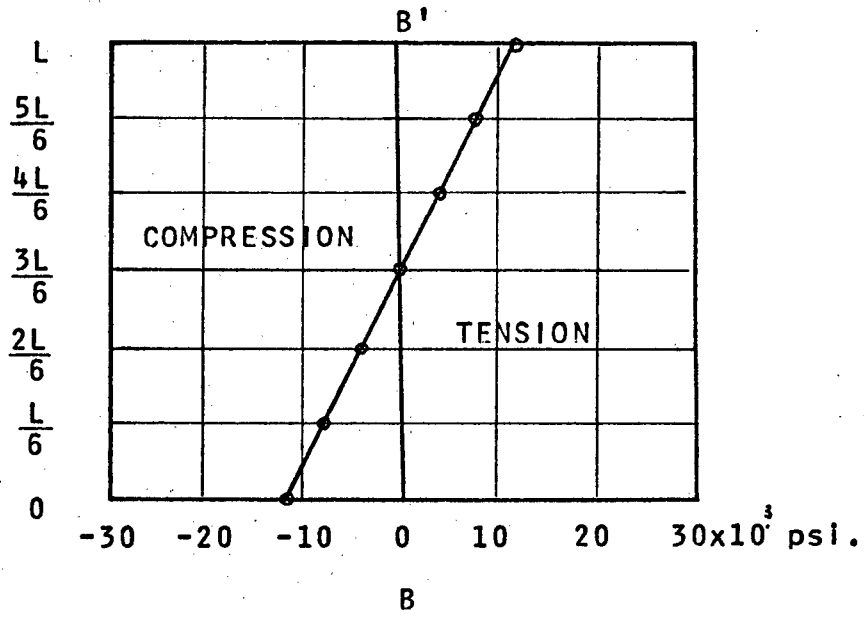


FIG.4-15a NORMAL STRESS DISTRIBUTION AT HIGHEST LOAD

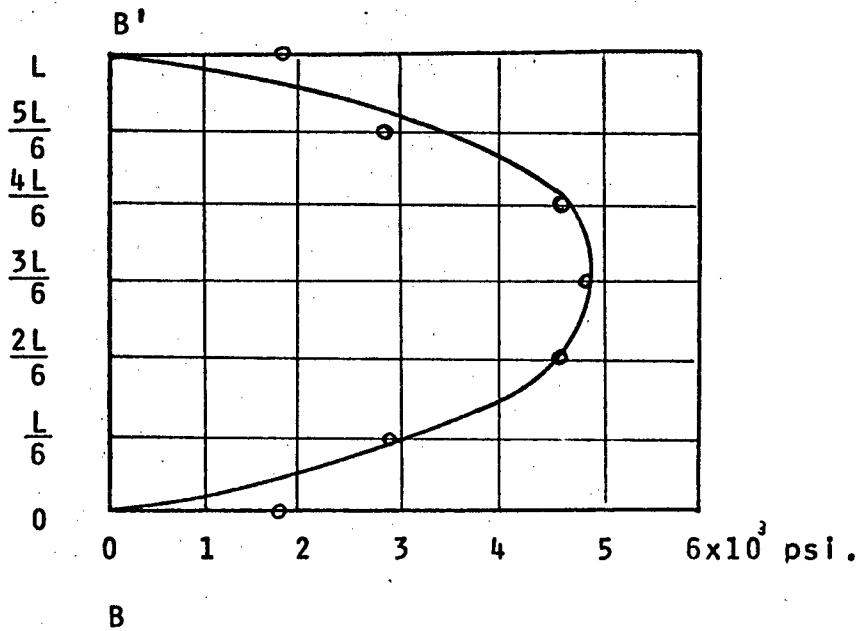


FIG.4-15b SHEAR STRESS DISTRIBUTION AT HIGHEST LOAD

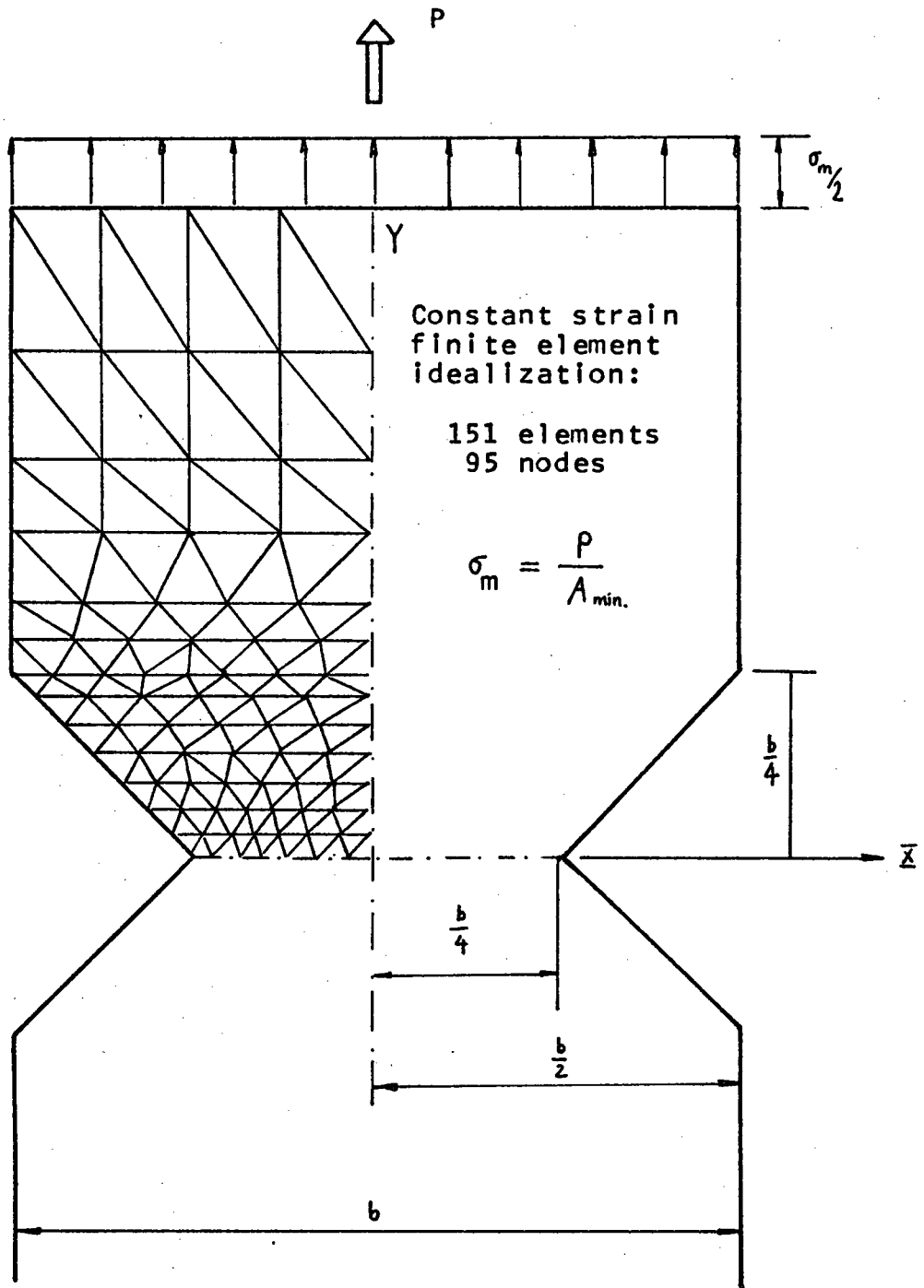
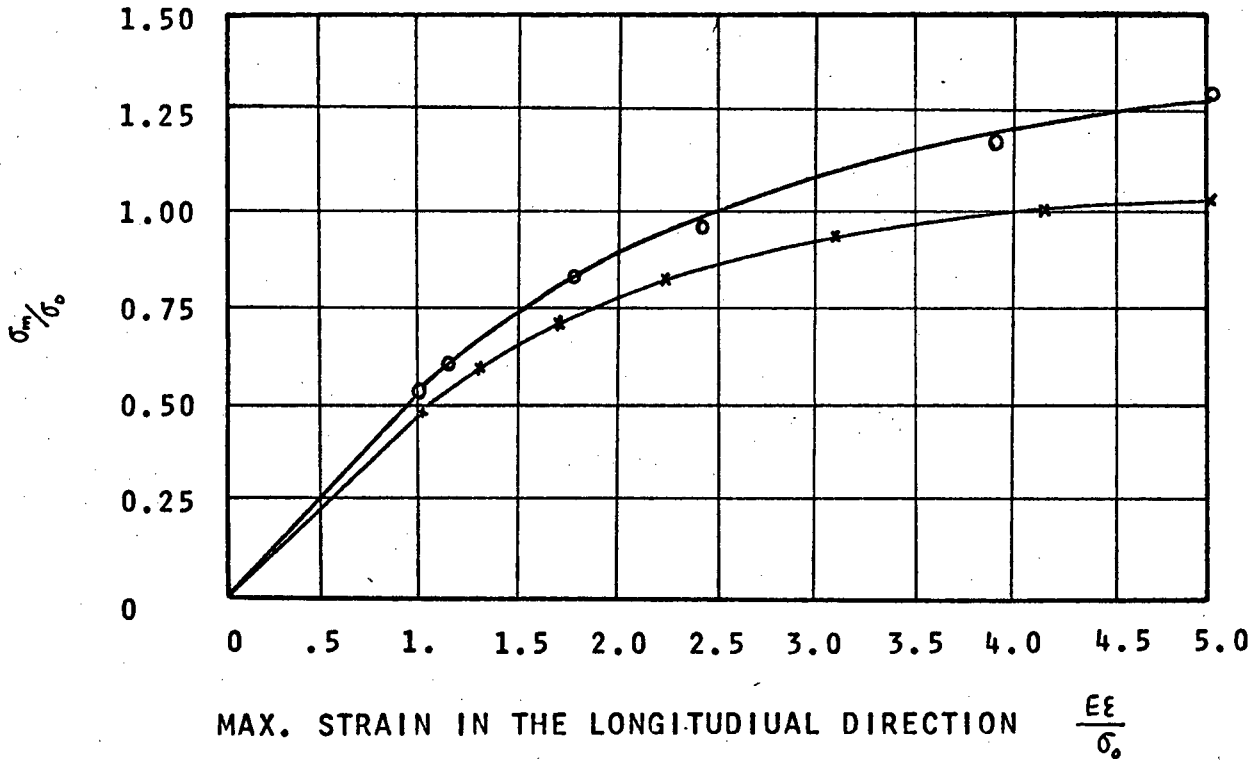


FIG.4-16 RIGHT-ANGLE NOTCH: ELASTIC-PERFECTLY-PLASTIC



- finite element solution for right angle notch
- × finite element solution for circular notch

FIG.4-17 END LOAD vs. MAX. STRAIN FOR NOTCHED TENSION SPECIMEN. ELASTIC-PERFECTLY-PLASTICITY

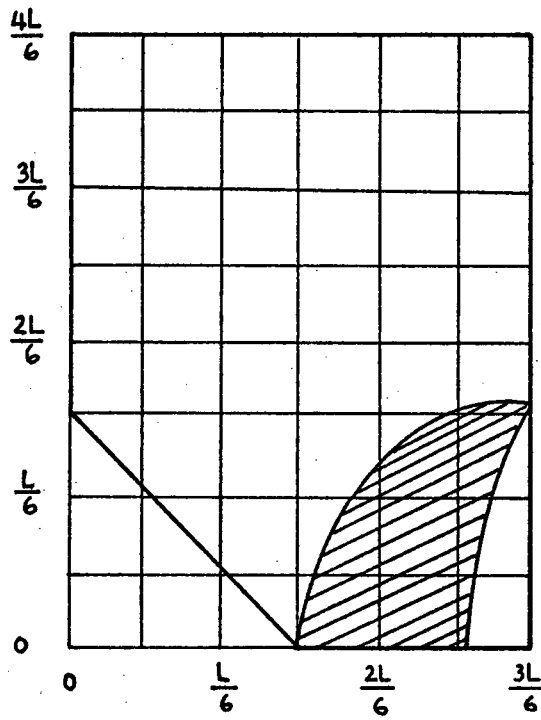


FIG.4-18a  
D. ALLEN & R. SOUTHWELL'S  
SOLUTION

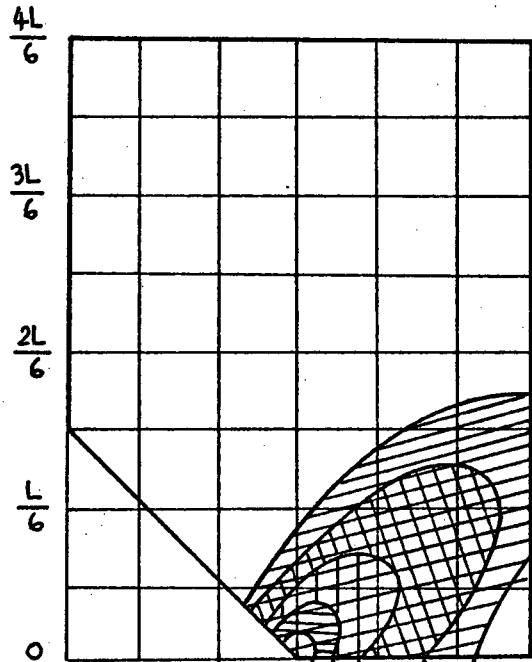


FIG.4-18b  
FINITE ELEMENT SOLUTION

$$\lambda = \begin{cases} 1.46 \\ 1.88 \\ 2.19 \\ 2.72 \\ 2.90 \end{cases}$$

## CHAPTER FIVE

### NONLINEAR STRESS ANALYSIS OF REINFORCED CONCRETE

#### 1. General Considerations

Studies of the nonlinear response to load of reinforced concrete structures have occupied the attention of many researchers during recent times. Because of the several complexities involved, however, the state variables of the concrete and steel are difficult to analyze. Some of the problems are stated below:

1. The nonhomogenous nature of the system.
2. The nonlinear behavior of the concrete and steel.
3. The structural system has a continuously changing character due to the influence of progressive cracking of the concrete under increasing load.
4. The possibility of relative movement between concrete and the steel reinforcement.
5. The deformations of concrete are influenced by creep and shrinkage and are time dependent.

The stress analysis of any solid body may be approached on a one, two or three-dimensional basis, and this is, of course, true for reinforced concrete. For example, if the

member is long compared with its depth and width, and if it remains uncracked, then beam theory is applicable. i.e. the usual one-dimensional analysis is satisfactory. After cracking, however, the one-dimensional analysis model fails completely. Thus, a realistic stress analysis of reinforced concrete must be based on at least a two-dimensional model. If the loads and the support reactions act only in a vertical plane, then the principal stress normal to this plane is considered to be very small compared with the others and a two-dimensional model is satisfactory.

Two-dimensional elasticity and plasticity could, indeed, be used to formulate the problem, but even then mathematical difficulties are encountered. The difficulties, however, can be overcome by the finite element method.

## II. Structural Idealization

In the application of the finite element method to reinforced concrete, the structure is decomposed into a number of regions, in each of which the behavior is represented by a separate field. Thus the nonhomogeneous nature of the construction can be accounted for. In this study, the well-known constant strain triangular elements have been used for the concrete. Perfect bond is assumed and the time dependent effect is also neglected. A displacement method of analysis under plane stress conditions has been used.



### III. Failure Criteria

a. Concrete:

1. Tensile crack: if the principal stress in any direction within an element exceeds the limiting tensile strength of concrete under uni-axial test, then the element is considered to have cracked perpendicularly to that principal direction.

2. Compressive yield: The Von Mises yield criterion has been used to define yield regions.

b. Steel: The Von Mises yield criterion has been used.

#### IV. Calculation Procedure

The subscripts and notations used here are the same as those in chapter four.

##### Procedure:

1. Compute  $[g]_0^n$
2. Compute  $[\Delta R]_{m+1}^n$
3. Compute  $\Delta \underline{\underline{\xi}}_{m+1}^{ne}$                        $\Delta \underline{\underline{\sigma}}_{m+1}^{ne}$
4. If the element has not cracked in previous steps, go to 6,
5. If the element has already cracked, then
  - a. Compute

$$\Delta \underline{\underline{\sigma}}' = [a_{pq}] \Delta \underline{\underline{\sigma}}_{m+1}^{ne} [a_{pq}]^T$$

where

$$[a_{pq}] = \begin{bmatrix} \cos \theta & -\sin \theta & 0 \\ \sin \theta & \cos \theta & 0 \\ 0 & 0 & 1 \end{bmatrix}$$

- b. Compute

$$\underline{\underline{\sigma}}'' = \underline{\underline{\sigma}}_m^n + \Delta \underline{\underline{\sigma}}'$$

- c. If the element cracked in                      direction (i.e.  $\sigma_2 \equiv 0$  ),  
then put

$\sigma_1 = \sigma_1''$	new value of the principal stress,
$\bar{\sigma}_2 = \sigma_2''$	residual principal stress(to be removed),
$\bar{\sigma}_1 = 0$	residual principal stress(to be removed),

and go to 12,

d. if the element cracked in  $\sigma_2$  direction (i.e.  $\sigma_1 \equiv 0$ ),  
then put

$\sigma_2 = \sigma_2^n$  new value of the principal stress

$\bar{\sigma}_1 = \sigma_1^n$  residual principal stress (to be removed)

$\bar{\sigma}_2 = 0$  residual principal stress (to be removed)

and go to 12,

6. Compute  $\underline{\sigma}_{m+1}^{ne}$ ,

7. Compute the principal stresses  $\sigma_1$  and  $\sigma_2$  and the principal direction  $\theta$  of  $\underline{\sigma}_{m+1}^n$ ,

8. If both  $\sigma_1$  and  $\sigma_2$  are less than the prescribed limiting tensile strength  $\sigma_{lt}$  then go to 11 to check yield.

9. If  $\sigma_1 \geq \sigma_{lt}$  then put

$$\bar{\sigma}_1 = \sigma_1,$$

$$\sigma_1 \equiv 0,$$

$$\bar{\sigma}_2 \equiv 0,$$

and go to 12,

10. If  $\sigma_2 \geq \sigma_{lt}$  then put

$$\bar{\sigma}_2 = \sigma_2,$$

$$\sigma_2 \equiv 0,$$

$$\bar{\sigma}_1 \equiv 0,$$

and go to 12,

11. Same procedure as given in chapter four:

a. if the element has yielded, then compute the residual stress  $\Delta \underline{\sigma}_{m+1}^{nr}$  and go to 13,

b. if not, then go to 1 starting with the next load increment.

12. compute the residual stress

$$\Delta \sigma_{m+1}^{nr} = [a_{pq}]^T [\bar{\sigma}] [a_{pq}]$$

where

$$[\bar{\sigma}] = \begin{bmatrix} \bar{\sigma}_1 & 0 & 0 \\ 0 & \bar{\sigma}_2 & 0 \\ 0 & 0 & 0 \end{bmatrix}$$

and  $[a_{pq}]$  is given in step 5,

13. compute the residual force  $[g]_{m+1}^n$

14. if  $\|[g]_{m+1}^n\| \ll \|[g]_0^n\|$ , then let

$$\underline{\sigma}_0^n = \underline{\sigma}_{m+1}^n$$

and go to 1 starting with next load increment,

15. if not, then compute the current stress and strain and go to 2 starting with next iteration.

#### IV. Numerical Example

##### Cantilever Beam

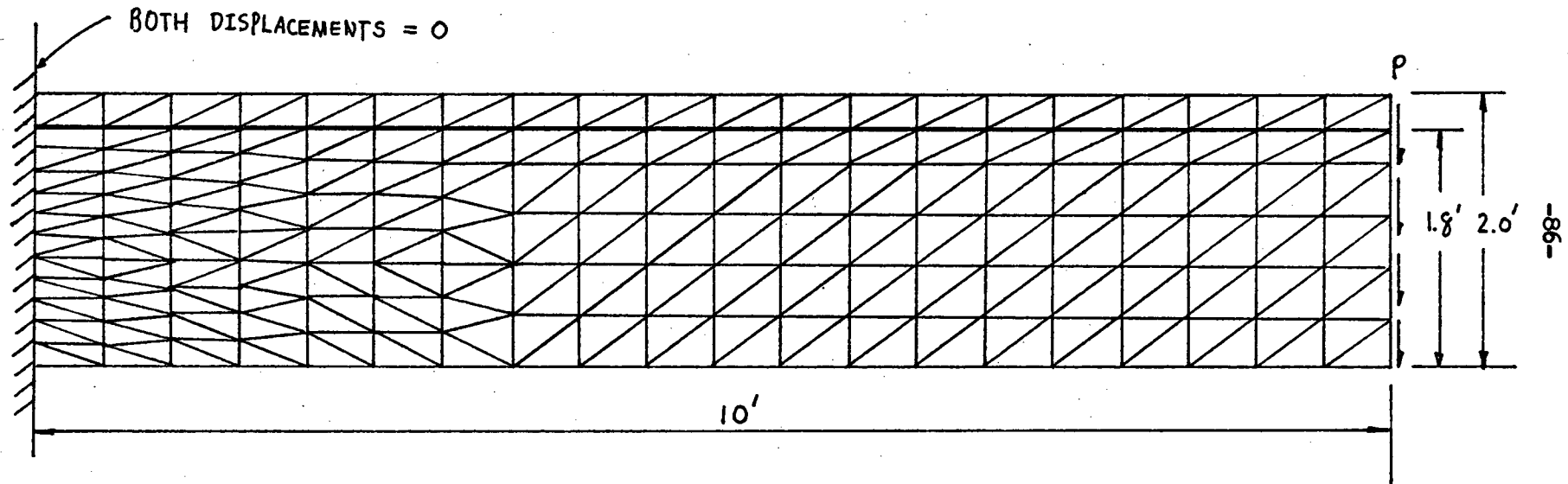
The structure that was studied is shown in Fig.5-1, in which the finite element net is presented. The material properties are shown in Fig.5-2.

An exact solution for this problem, within the assumption of plane sections remaining plane, could be obtained by manipulation of the equilibrium equations based on Fig.5-3, and the results are shown in Fig.5-4.

Stages of the finite element solution are shown in Fig. 5-5 to 5-11. For a given moment, the extreme fibre strain of the concrete and the neutral axis depth for the "exact" solution can be obtained from Fig.5-4, and the corresponding stress distributions are shown on Fig.5-5 to 5-8 for comparison.

It will be seen that the results are in reasonable agreement up to this stage, but that the finite element solution shows the load increasing well beyond the actual maximum. Fig.5-4 shows that the load capacity of the structure has actually levelled off at a moment of 170.6 Kft., and the program is clearly failing to converge properly under these conditions.

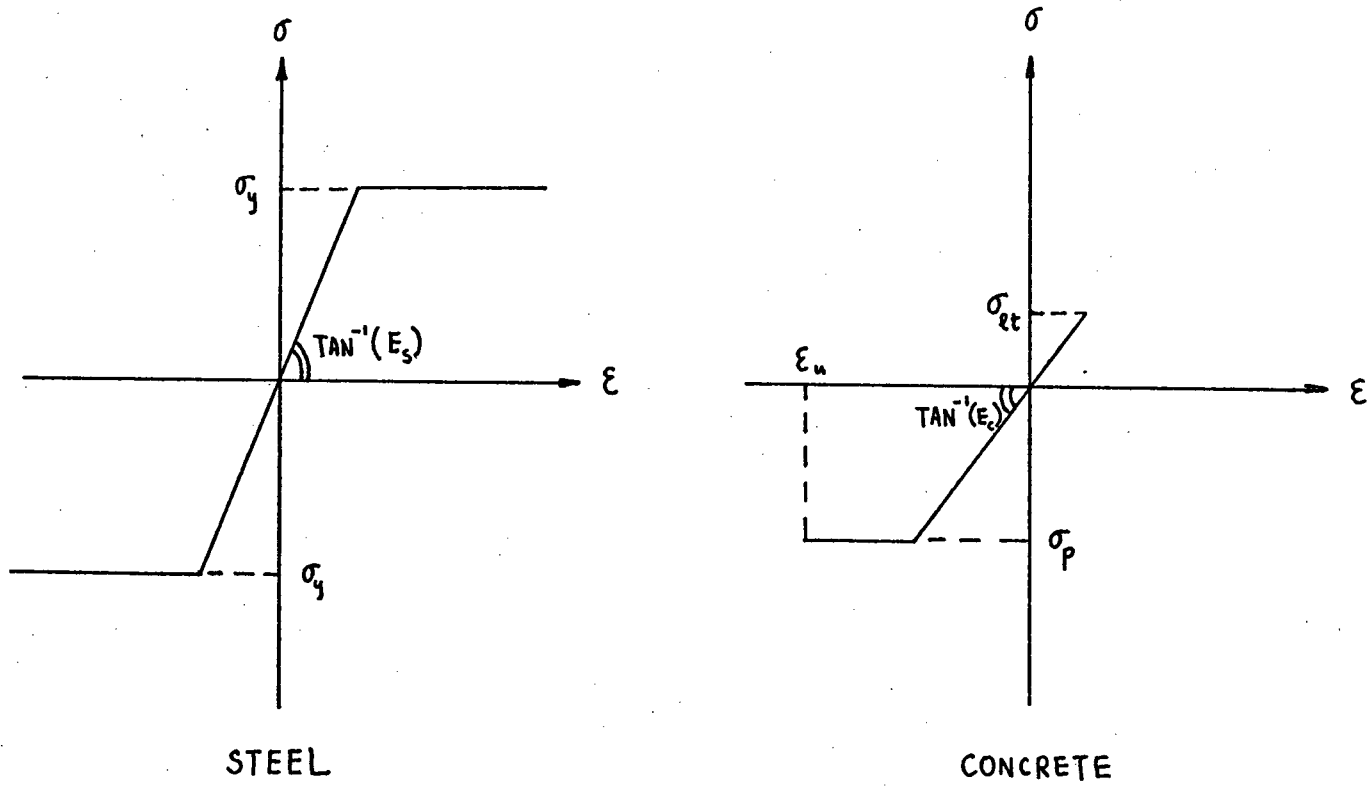
Fig.5-12 shows the cracking pattern and the plastic region which develops in the beam. These are believed to be representative of the truth.



$$A_s = 2.54 \text{ in}^2$$

THICKNESS = 12 in.

FIG.5-1 REINFORCED CONCRETE CANTILEVER BEAM



$$\sigma_y = 40.00 \text{ ksi.}$$

$$\sigma_p = 3.00 \text{ ksi.}$$

$$\sigma_{pt} = 0.42 \text{ ksi.}$$

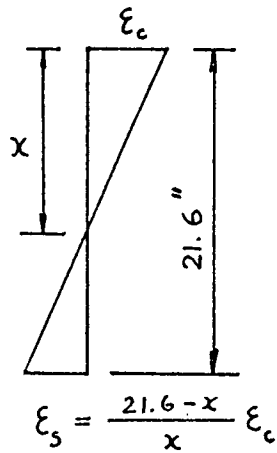
$$E_s = 29 \times 10^3 \text{ ksi.}$$

$$E_c = 3.1 \times 10^3 \text{ ksi.}$$

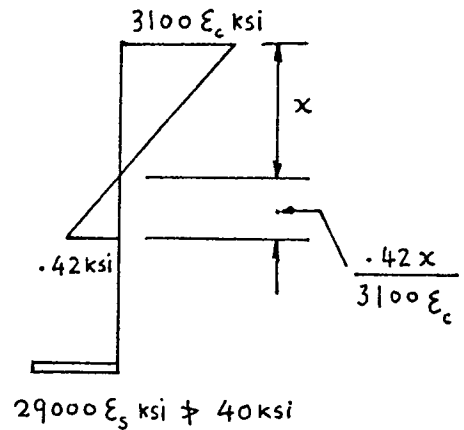
$$\epsilon_u = 0.003$$

FIG.5-2 UNIAxIAL STRESS-STRAIN CURVES

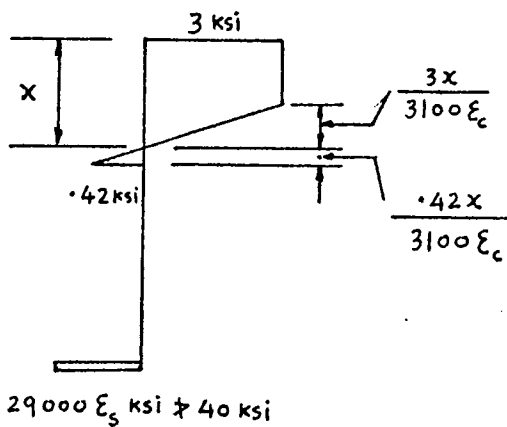




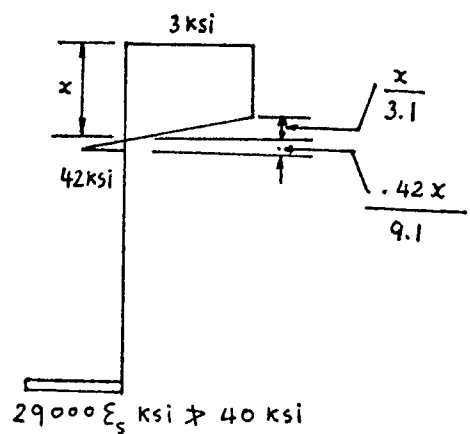
Strain Diagram



Stress Diagram ( $\epsilon_c \leq .000968$ )



Stress Diagram ( $\epsilon_c > .000968$ )



Stress Diagram ( $\epsilon_c = 0.003$ )

$$\text{STEEL FORCE} = T = 73660 \frac{21.6 - x}{x} \epsilon_c \neq 101.6 \text{ kips}$$

$$\text{CONCRETE FORCE} = C = \left( 18600 \epsilon_c x - 3.414 \times 10^{-4} \frac{x}{\epsilon_c} \right) \text{ kips}, \quad \epsilon_c \leq .000968$$

$$= \left( 36x - 1.74 \times 10^{-2} \frac{x}{\epsilon_c} - 3.414 \times 10^{-4} \frac{x}{\epsilon_c} \right) \text{ kips}, \quad \epsilon_c > .000968$$

$$= 30.08 x \text{ kips}, \quad \epsilon_c = .003$$

FIG. 5-3.

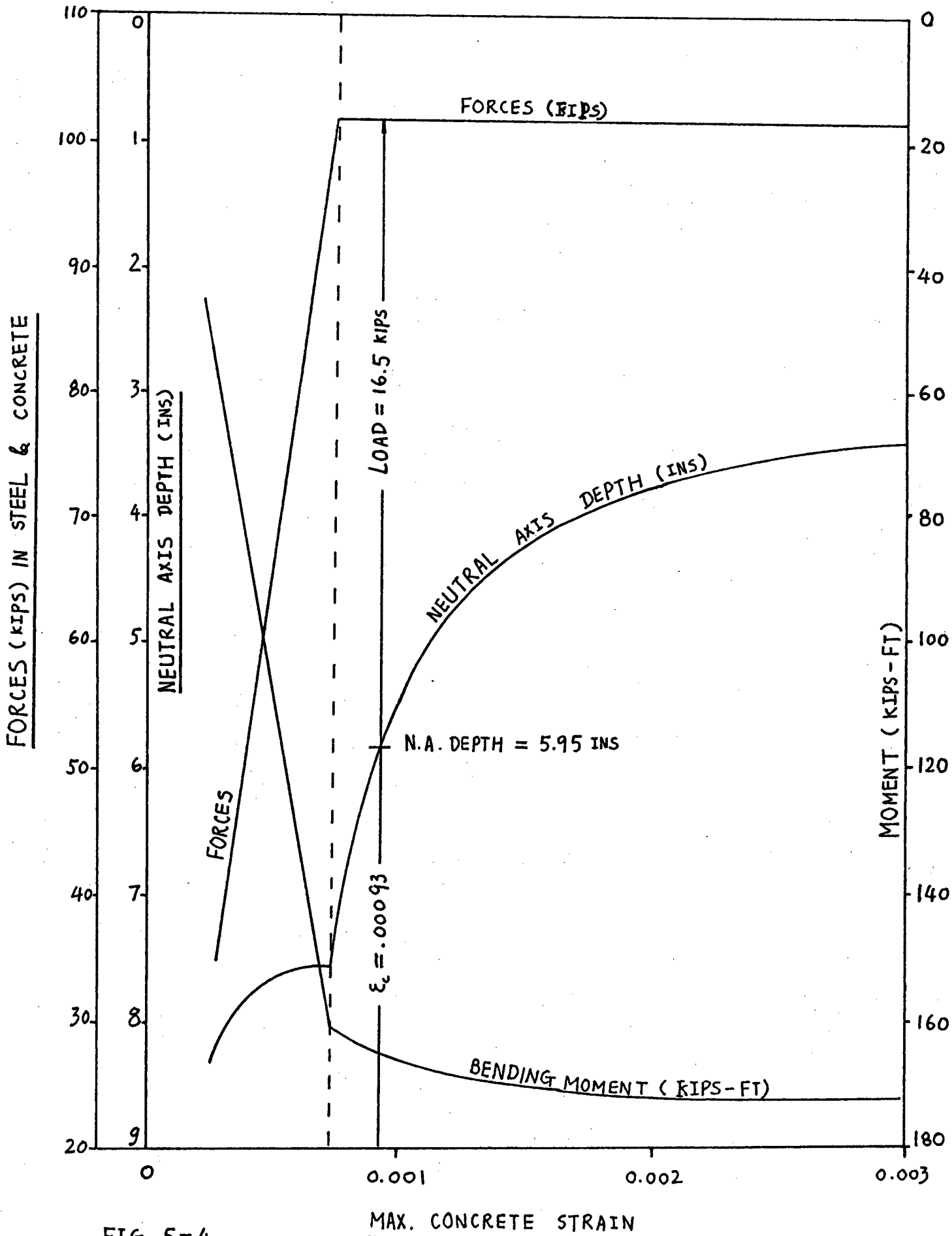


FIG. 5-4

P = 11 kips.

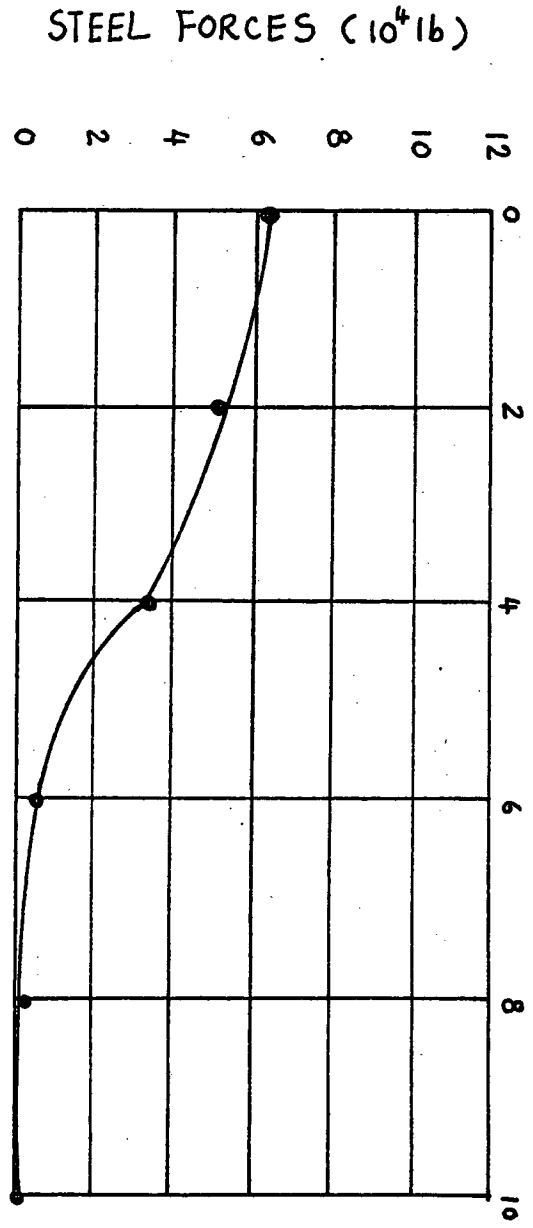
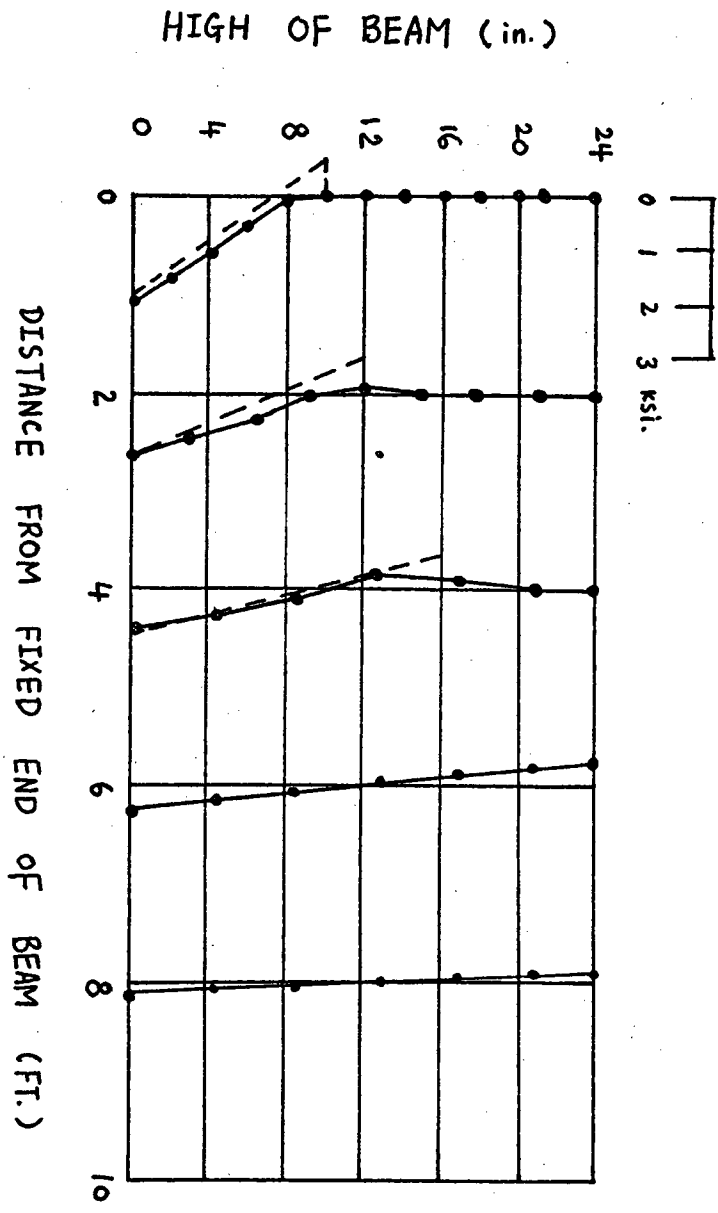
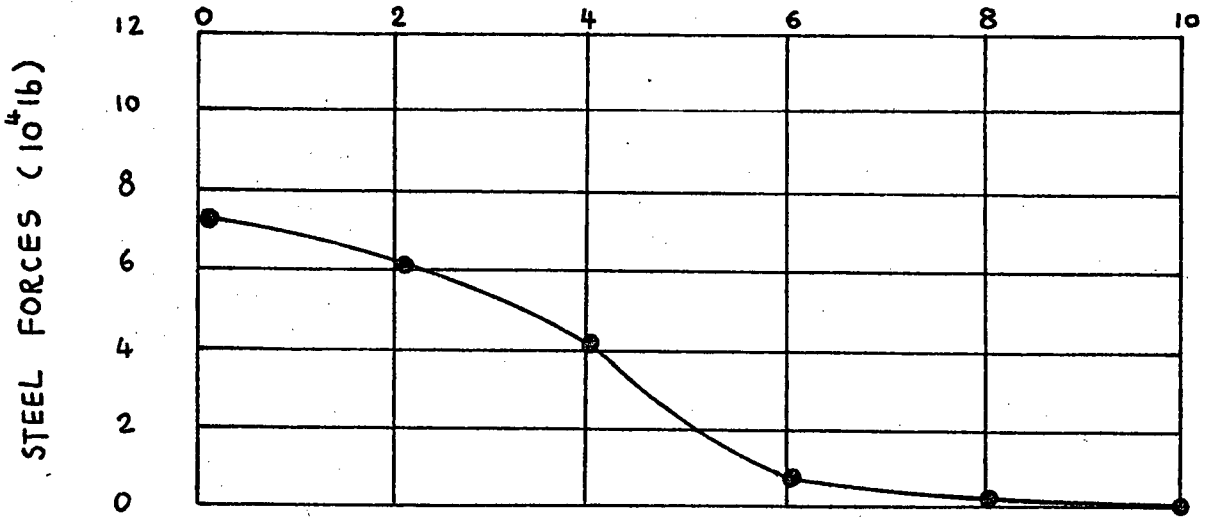
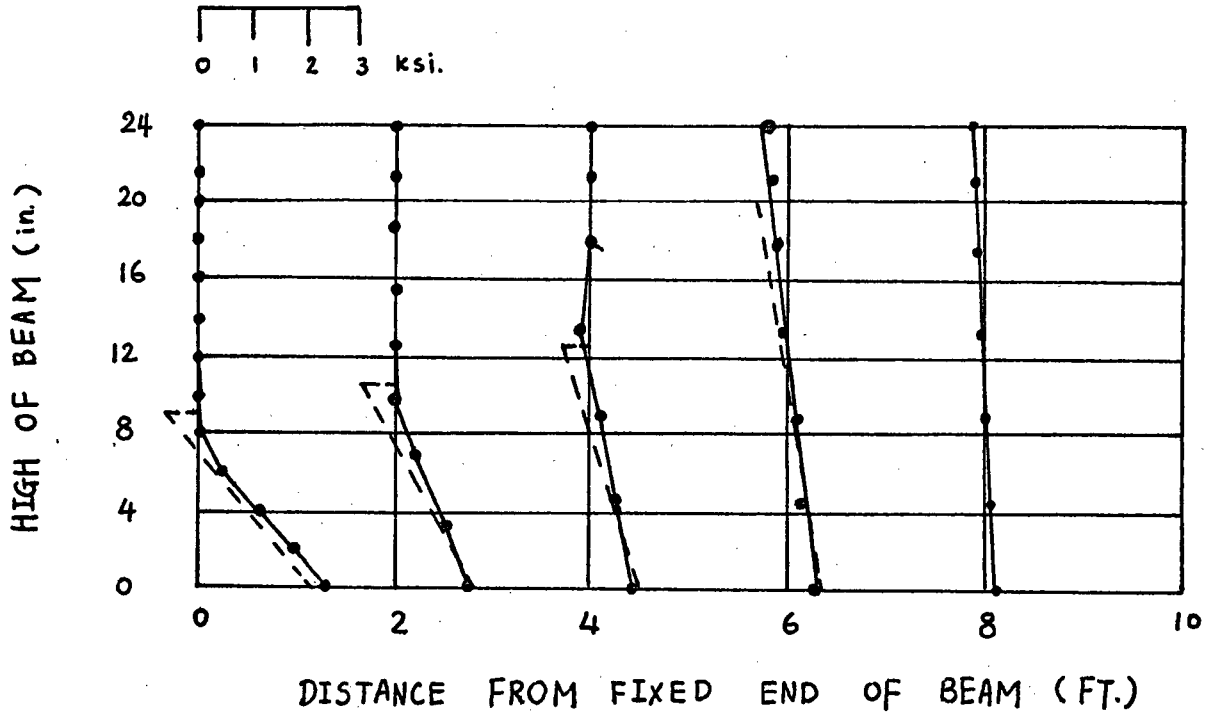


Fig. 5-5

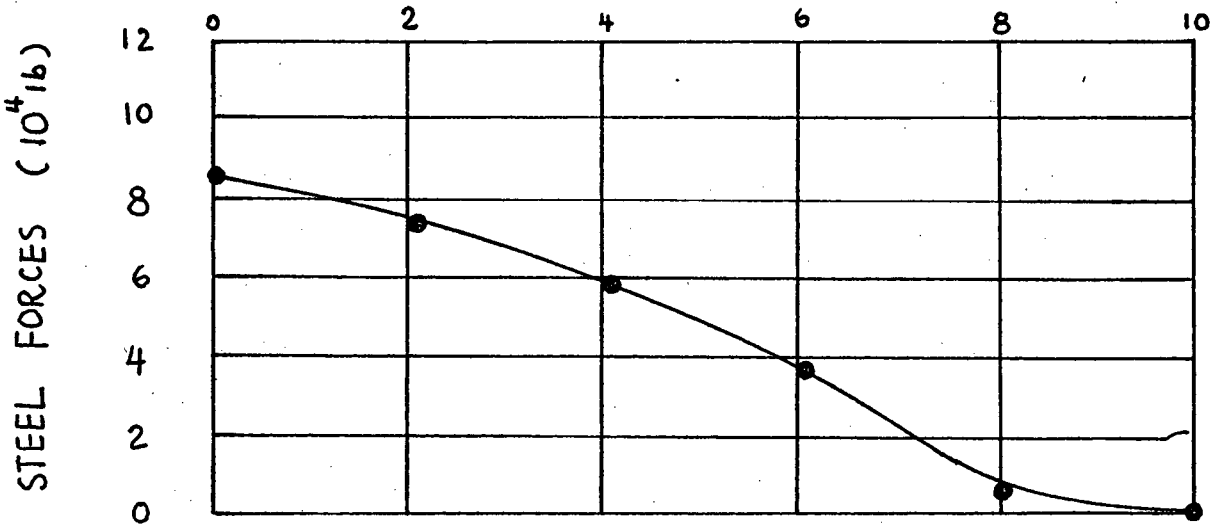
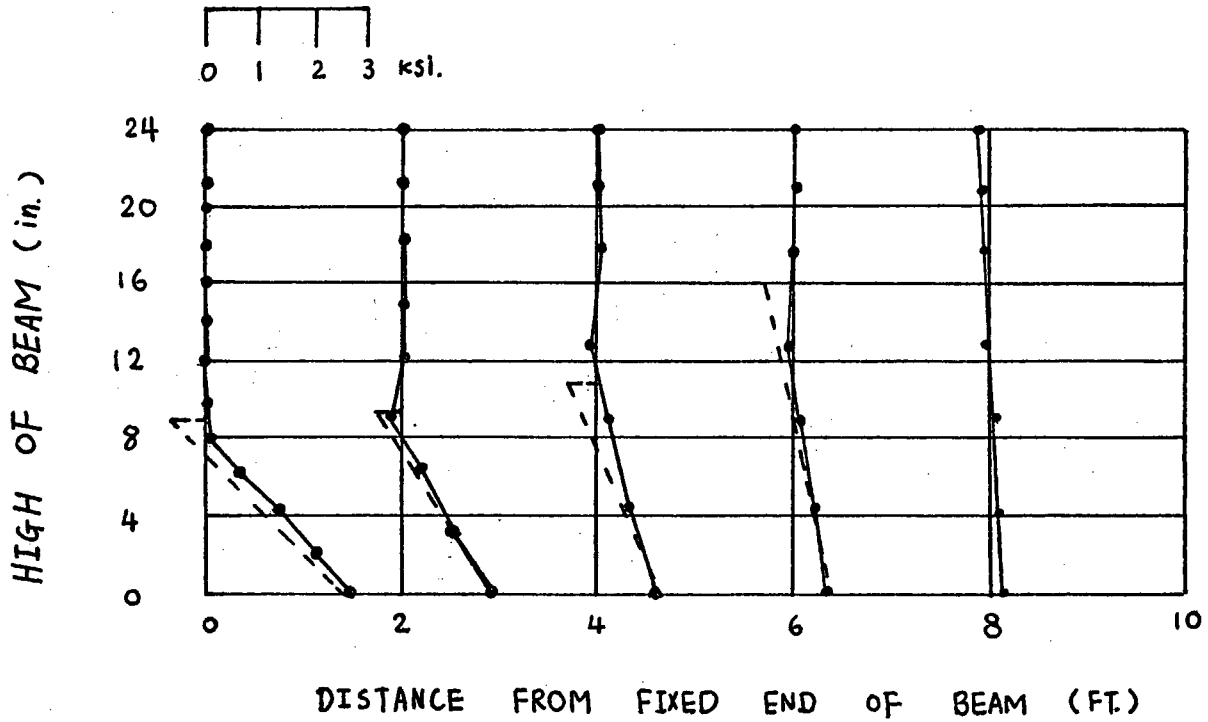
$P = 13$  kips.



———— Computed values  
----- Theoretical values

Fig. 5-6

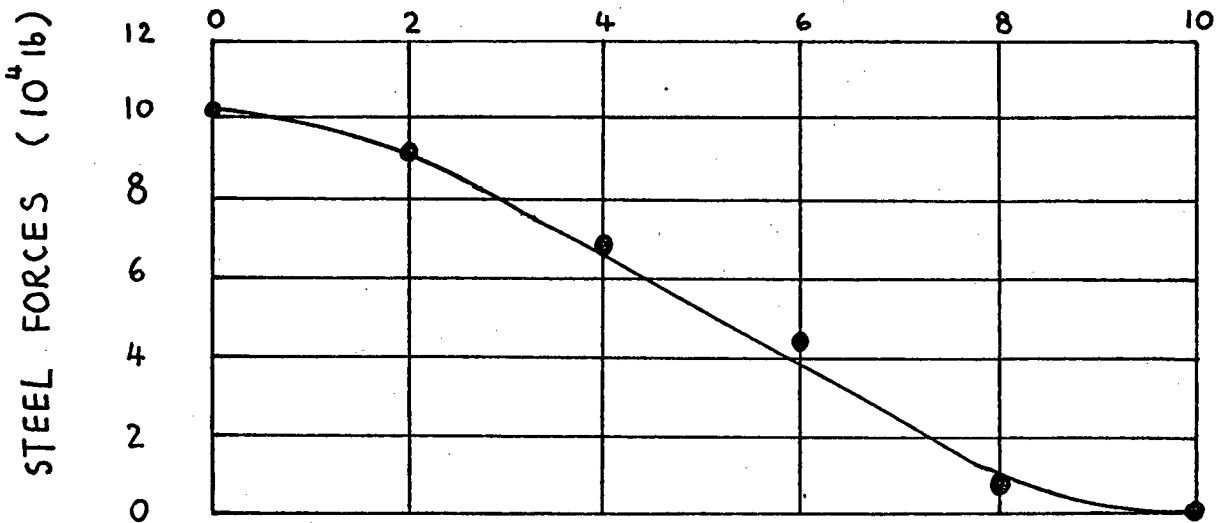
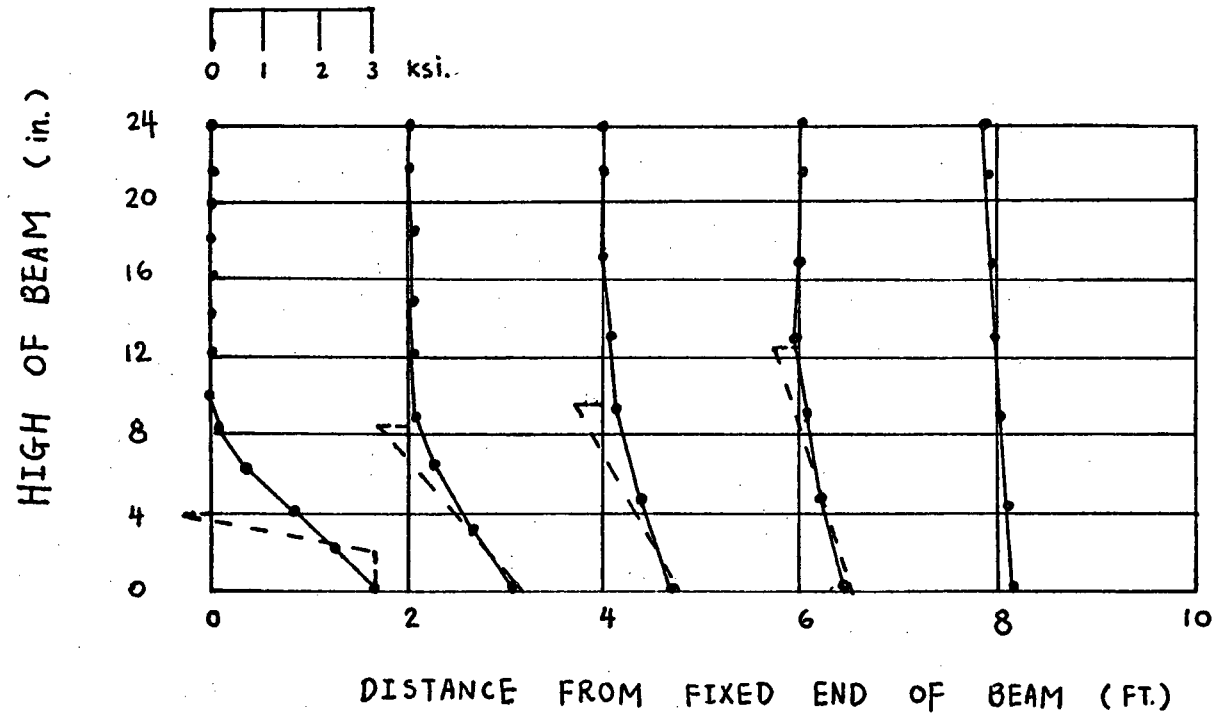
P = 15 KIPS.



———— Computed values  
----- Theoretical values

Fig. 5-7

$P = 17$  KIPS.



———— Computed values  
----- Theoretical values

Fig. 5-8

$P = 20$  kips.

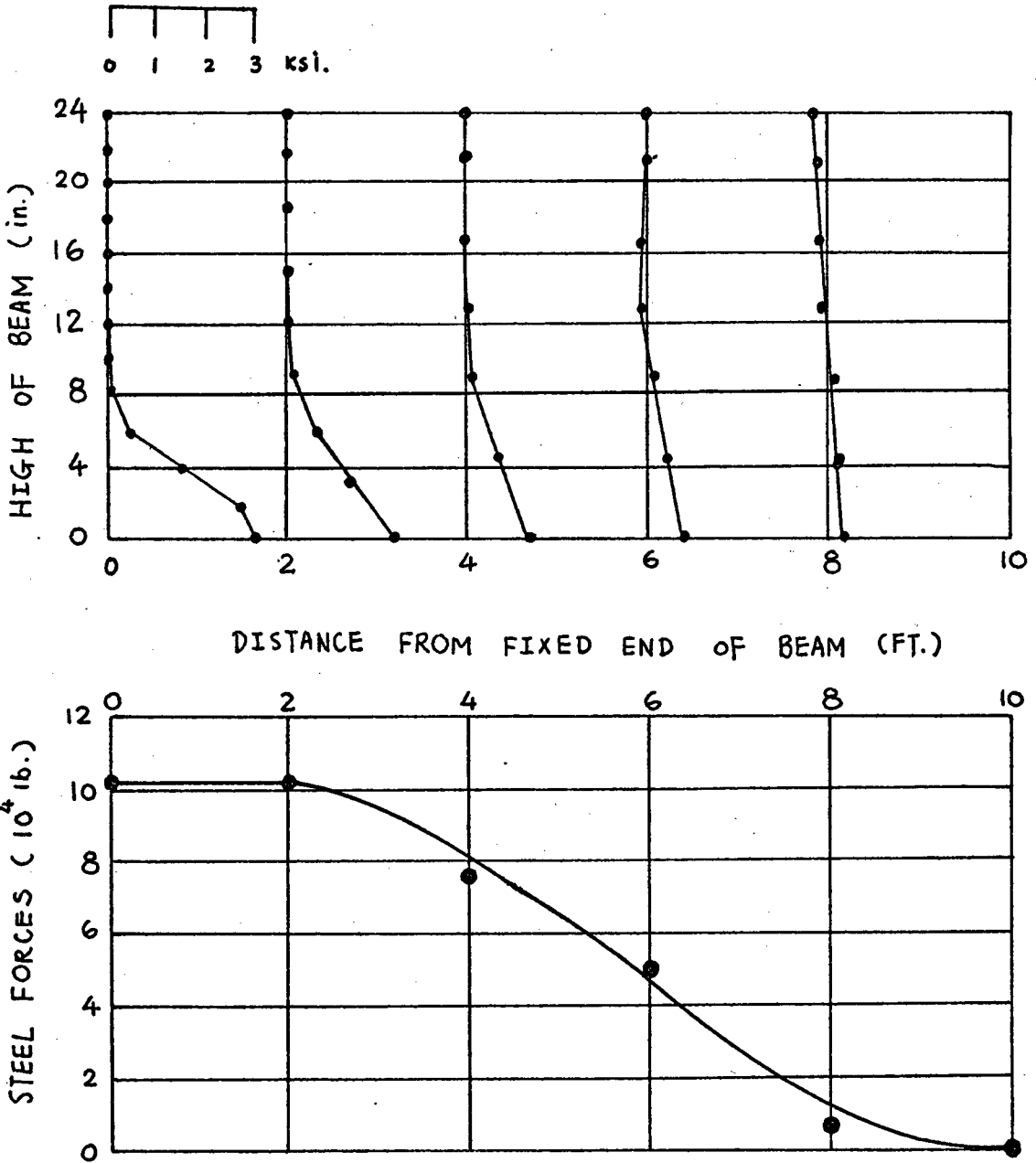


FIG. 5-9

$P = 24$  KIPS.

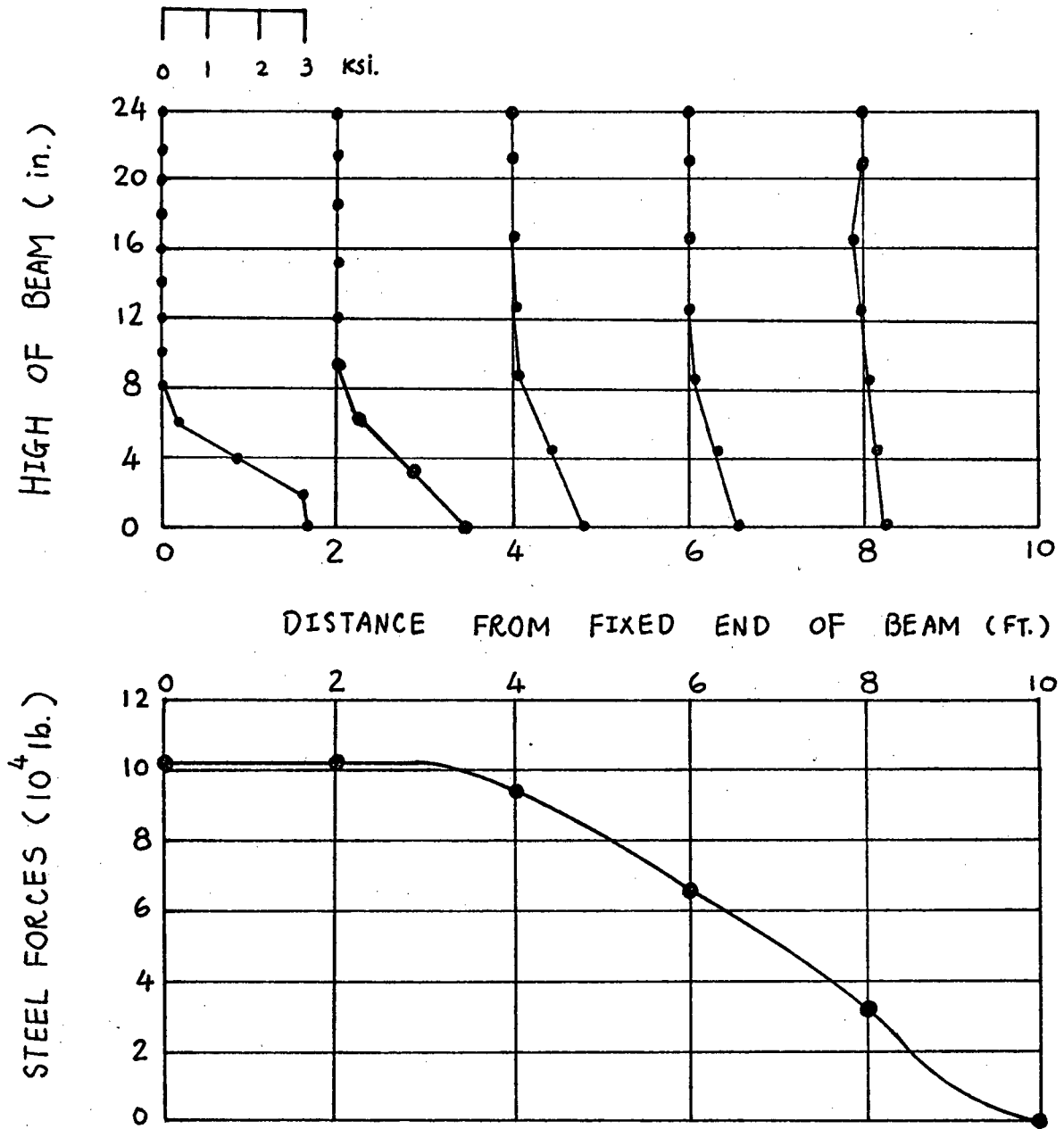


FIG. 5-10



$P = 26$  kips.

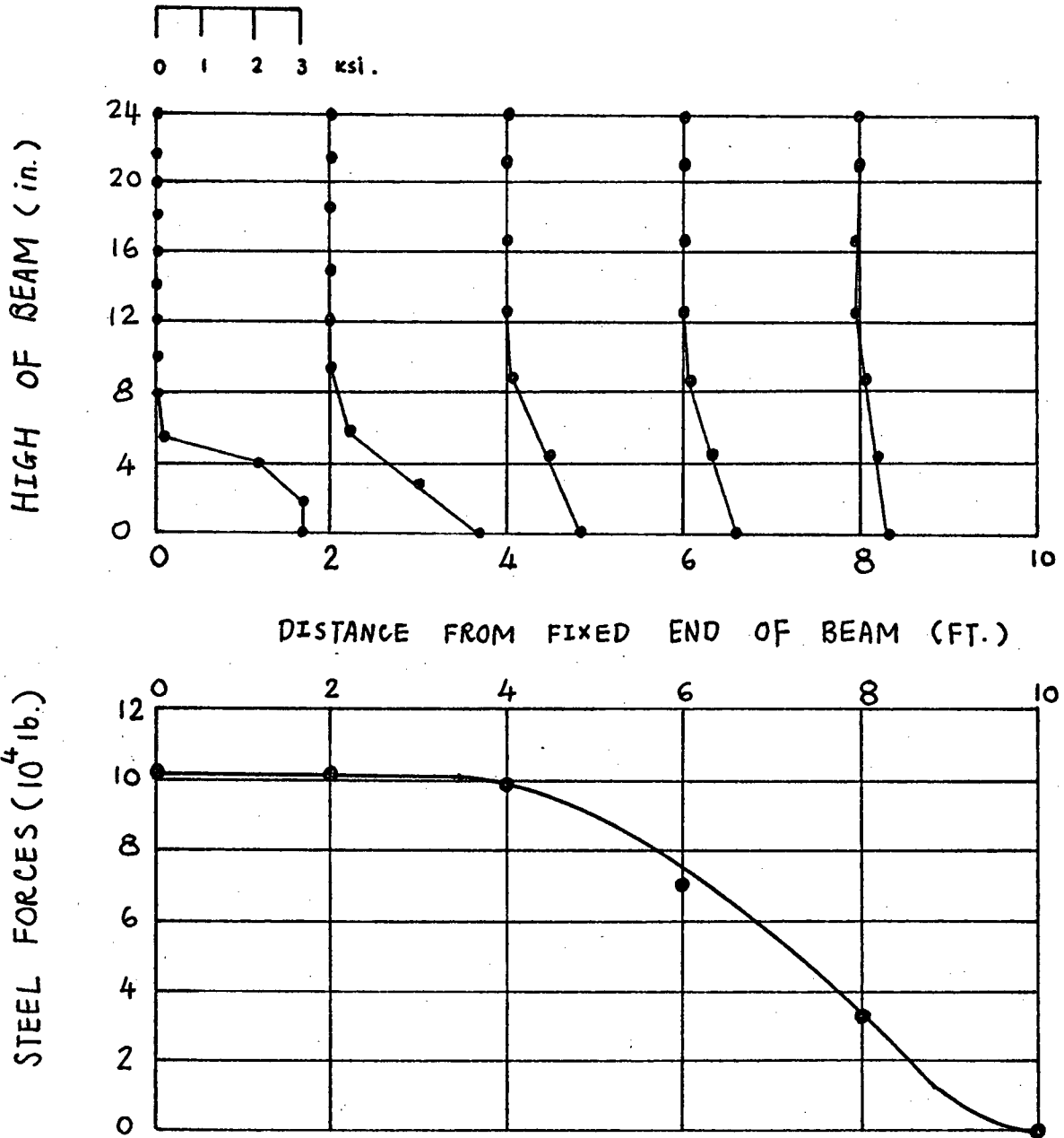


FIG. 5-11

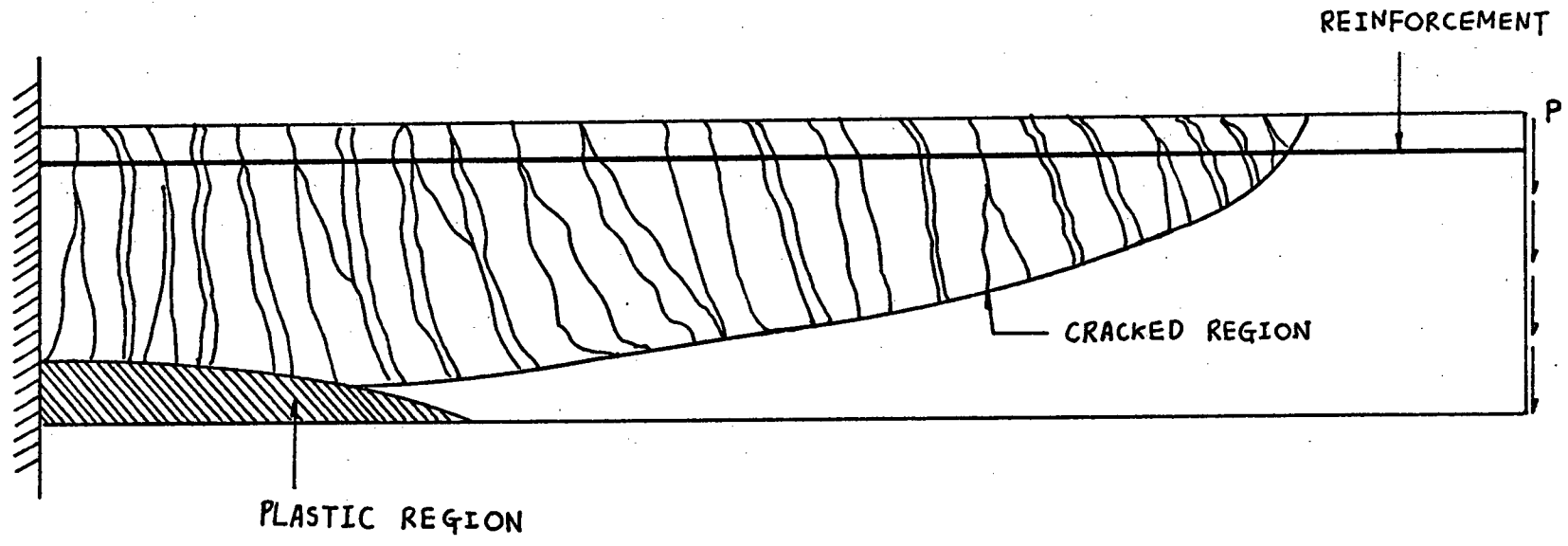


FIG.5-1Z PLASTIC REGION, CRACKED REGION

## CHAPTER SIX

### Conclusions

A nonlinear finite element program has been developed to obtain the elasto-plastic stress and strain distribution in a plane stress continuum composed of a perfectly plastic and a linear strain-hardening material.

Since the program is based on D.C. Drucker's definition, it is very general and good for any criterion or for different forms of hardening rule.

A combination of the load increment technique and the modified Newton-Raphson method was used to solve the nonlinear equilibrium equation and shown to be practical and economical in computer time. For collapse investigations, this procedure is non-convergent or converges very slowly; this is clearly a result of the iterative technique. Furthermore, it is known that when a large proportion of the region becomes plastic the convergence may be slow.

The program was extended to deal with reinforced concrete members; for the concrete, a bilinear elastic-perfectly plastic curve was assumed for comparison and an elastic curve up to cracking in tension; a bilinear elastic-perfectly plastic curve was used for the steel. It was found that stress and crack distribution could be predicted with reasonable accuracy until the ultimate moment was approached. It appeared that the iterative method failed to converge successfully at the yield moment. It is possible that an elastic-strain hardening curve for the concrete might have extended the usefulness of these results.

APPENDIX

THE PRINCIPLE OF MINIMUM POTENTIAL ENERGY FOR THE INCREMENTAL FORMULATION

A brief mention is made here concerning the principle of stationary potential energy applied to nonlinear problems in solid mechanics. As stated earlier, the incremental theory is frequently employed in the analysis of nonlinear problems, thus it is necessary to expand the principle to permit the determination of an incremental state superimposed upon a body with an existing equilibrium stress state.

Let us consider that the loads on the body are increased monotonically, and denote the states of the body as  $G_1, G_2, G_3, \dots, G_m, G_{m+1}, \dots$  we assume that the  $G_m$ -state has been found and we want to have an incremental formulation (incremental equilibrium equation) for the analysis of the  $G_{m+1}$  -state. This increment from  $G_m$  to  $G_{m+1}$  is small enough to allow linearization of all the field equations w.r.t. the incremental quantities. For this case, we may write the potential energy functional for the  $G_{m+1}$  state as follows

$$\begin{aligned} V_p = V_p^m + V_p^{m+1} = & \sum_n \left[ - \int_{S_{\sigma_n}} (T_i^m + \Delta T_i)(u_i^m + \Delta u_i) dS \right. \\ & - \int_{V_n} (F_i^m + \Delta F_i)(u_i^m + \Delta u_i) dV \\ & \left. + \int_{V_n} (W^m + \Delta W) dV \right] \end{aligned} \quad (A-1)$$

where the internal energy function  $W$  is a function of stresses or of strains. For the present, let us take

$$W = w(\varepsilon_{ij}) \quad (A-2)$$

Then

$$dW = \frac{\partial W}{\partial \varepsilon_{ij}} d\varepsilon_{ij} \quad (A-3)$$

One form of the first law of thermodynamics for a continuous medium, where heat transfer terms are neglected and displacement gradients are assumed small, may be written:

$$dW = \sigma_{ij} d\varepsilon_{ij} \quad (A-4)$$

and Eq.(A-3) may be written as

$$\left( \sigma_{ij} - \frac{\partial W}{\partial \varepsilon_{ij}} \right) = 0 \quad (A-5)$$

Noting that Eq.(A-5) must be an identity for any arbitrary  $d\varepsilon_{ij}$ , we deduce that the coefficient of  $d\varepsilon_{ij}$  must vanish, i.e.

$$\frac{\partial W}{\partial \varepsilon_{ij}} = \sigma_{ij} \quad (A-6)$$

or

$$\Delta \left( \frac{\partial W}{\partial \varepsilon_{ij}} \right) = \frac{\partial^2 W}{\partial \varepsilon_{ij} \partial \varepsilon_{kl}} \Delta \varepsilon_{kl} = \Delta \sigma_{ij} \quad (A-7)$$

By Taylor's Theorem, the increment of the internal energy function  $\Delta W$  corresponding to increments  $\Delta \varepsilon_{ij}$  of the  $\varepsilon_{ij}$  is

$$\Delta W = \Delta \varepsilon_{ij} \frac{\partial W}{\partial \varepsilon_{ij}} + \frac{1}{2!} \Delta \varepsilon_{ij} \Delta \varepsilon_{kl} \frac{\partial^2 W}{\partial \varepsilon_{ij} \partial \varepsilon_{kl}} + \dots \quad (A-8)$$

Substituting Eqs.(A-6) and (A-7) into (A-8), gives

$$\Delta W = \Delta \varepsilon_{ij} \sigma_{ij} + \frac{1}{2} \Delta \varepsilon_{ij} \Delta \sigma_{ij} \quad (\text{A-9})$$

Expanding Eq.(A-1), in view of Eq.(A-9), leads to

$$\begin{aligned} V_p = V_p^m + V_p^{m'} &= \sum_n \left[ - \int_{S_{\sigma_n}} T_i^m u_i^m ds - \int_{V_n} F_i^m u_i^m dV + \int_{V_n} w^m dV \right] \\ &+ \sum_n \left[ - \int_{S_{\sigma_n}} T_i^m \Delta u_i ds - \int_{V_n} F_i^m \Delta u_i dV + \int_{V_n} \sigma_{ij}^m \Delta \varepsilon_{ij} dV \right] \\ &+ \sum_n \left[ - \int_{S_{\sigma_n}} \Delta T_i (u_i^m + \Delta u_i) ds - \int_{V_n} \Delta F_i (u_i^m + \Delta u_i) dV + \int_{V_n} \frac{1}{2} \Delta \varepsilon_{ij} \Delta \sigma_{ij} dV \right] \end{aligned} \quad (\text{A-10})$$

Since the  $G_m$ -state is in equilibrium, the principle of virtual displacements leads to:

$$\sum_n \left[ - \int_{S_{\sigma_n}} T_i^m \Delta u_i ds - \int_{V_n} F_i^m \Delta u_i dV \right] + \sum_n \int_{V_n} \sigma_{ij}^m \Delta \varepsilon_{ij} dV = 0 ,$$

and we have

$$\begin{aligned} V_p = V_p^m + \sum_n \left[ - \int_{S_{\sigma_n}} \Delta T_i (u_i^m + \Delta u_i) ds - \int_{V_n} \Delta F_i (u_i^m + \Delta u_i) dV \right. \\ \left. + \int_{V_n} \frac{1}{2} \Delta \varepsilon_{ij} \Delta \sigma_{ij} dV \right] . \end{aligned} \quad (\text{A-11})$$

Taking variations of Eq.(A-11) w.r.t. all admissible incremental displacement fields leads to the variational principle:

$$\delta V_p = \delta \left\{ \sum_n \left[ - \int_{S_{\sigma_n}} \Delta T_i \Delta u_i dS - \int_{V_n} \Delta F_i \Delta u_i dV + \frac{1}{2} \int_{V_n} \Delta \sigma_{ij} \Delta \varepsilon_{ij} dV \right] \right\} = 0$$

or in matrix form

(A-12a)

$$\delta V_p = \delta \left\{ \sum_n \left[ - \int_{S_{\sigma_n}} \Delta \underline{T}^T \Delta \underline{u} dS - \int_{V_n} \Delta \underline{F}^T \Delta \underline{u} dV + \frac{1}{2} \int_{V_n} \Delta \underline{\sigma}^T \Delta \underline{\varepsilon} dV \right] \right\} = 0$$

(A-12b)

It is interesting to note that Eq.(A-12) has the same form as the linear elastic case, Eq.(3-7), except that all the state variables  $T, u, F, \sigma, \varepsilon$  are now in incremental forms.



BIBLIOGRAPHY

1. V.V. Novozhilov: Foundations of Nonlinear Theory of Elasticity Graylock Press, Rochester, N.Y., 1953. P.128
2. O.C. Zienkiewicz: The Finite Element Method in Engineering Science, McGraw-Hill, London, 1971.
3. N.D. Nathan: Finite Element Formulation of Geometrically Non-linear Problems of Elasticity, Japan-U.S. Seminar on Matrix Methods of Structural Analysis and Design, Tokyo 1969, pp. 415-437.
4. R.H. Gallagher: Stress Analysis of Heated Complex Shapes, J. Am. Rocket Soc. 32,1962. pp 700-707
5. A. Mendelson: Practical solution of Plastic Deformation Problems in the Elastic -plastic Range, NASA TRR28, 1959.
6. J.H. Argyris: Matrix Methods of Structural Analysis. A Precs of Recent Developments Proceedings, Fourteenth Meeting of Structures and Materials Panel, AGARD, 1963.
7. J.H. Percy: A Study of Matrix Analysis Method for Inelastic Structures, RTD-TDR-63-4032, October 1963.
8. W.R. Jensen: Matrix Analysis methods for Anisotropic Inelastic Structures, AFFDL-TR-65-220, 1966.
9. P.V. Marcal: Comparative Study of Numerical Methods of Elastic-Plastic Analysis, AIAA J. Vol. 6, No.1, 1967, pp.157-58.
10. G. Pope: The application of the matrix displacement method in plane elasto-plastic problems, Proc. Conf. Matrix Meth. Struct. Mech. Wrigh-Patterson Air Force Base, Ohio, 1965 pp.635-54.
11. T.L. Swedlow: Elasto-plastic stresses in Cracked Plates, Calcit, Report SM, 65-19, Californis Institute of Technology, 1965.
12. S.F. Reys: Elasto-plastic Analysis of Underground Openings by the Finite Element Method, Proc. 1st. Int. Congr. Rock Mechanics, 11,477-86, Lisbon 1966.
13. P.V. Marcel: Elastic-plastic analysis of two dimensional Stress Systems by the Finite Element Method, Int. L. Mech Sci., 9, 143-55, 1967.
14. Y. Yamada: Stiffness Matrix In Plastic-elastic Problems of Continua, Seisan Kenkyn (monthly J. of Institute of Industrial Science), Vol. 19, No.3, 1967, pp. 75-76.

15. O.C. Zienkiewicz: Elasto-plastic Solutions of Engineering Problems "initial stress", Finite Element Approach. Int. J. Num. Meth. Engineering, 1, 75-100, 1969
16. Y. Yamada: Recent Japanese Developments in Matrix Displacement Method of Elastic-plastic problems, Japan-U.S. Seminar on Matrix Methods of Structural Analysis and Design, Tokyo, 1969.
17. R. Hill: The Mathematical Theory of Plasticity, Oxford, Univ. Press, 1950. P. 317.
18. G.C. Nayak: Elasto-plastic Stress Analysis. A Generalization for various Constitutive relations including strain Softening, Int. J. Num. Meth. Engng. 5, 113-35, 1972.
19. S. Timoshenko and J.N. Goodier: Theory of Elasticity, MacGraw-Hill Book Co. Inc., N.Y., 1951, p.4.
20. H. Jeffreys: Cartesian Tensors, Cambridge, Univ. Press, 1931.
21. Y.C. Fung: Foundations of Solid Mechanics, Prentice-Hall, Inc., N.J., 1965, p.100.
22. I.S. Sokolnikoff: Mathematical Theory of Elasticity, McGraw-Hill Book Co. Inc., N.Y. 1956. p.66.
23. C.E. Pearson: Theoretical Elasticity, Cambridge, Mass. Harvard Univ. Press, 1959. p. 97.
24. Y.C. Fung: Foundations of Solid Mechanics, Prentice-Hall, Inc., N.J., 1965 p. 137.
25. W. Johnson: Plasticity for Mechanical Engineering, VAN Nostrand Co., Ltd. London 1962. p.62.
26. A. Mendelson: Plasticity-Theory and Application, Macmillan, N.Y. 1968. p.104.
27. R. Hill: The Mathematical Theory of Plasticity, Oxford, Press, 1950. p. 39.
28. D.C. Drucker: Some Implication of Work Hardening and Ideal Plasticity, Quart. Appl. Math., 7, 1950, pp.411-18.
29. D.C. Trucker: Handbook of Engineering Mechanics, Chapter 46, 1962.
30. E.R. Oliveira: Theoretical Foundations of the Finite Element Method, Internal J. Solids Structures. 1968. Vol.4 pp.929-952.

31. T.H. Pian and P. Tong: Basic of Finite Element Methods for Solid Continua, Int. J. for Num. Meth. in Eng. Vol.1, 3-28, 1969.
32. R.H. Gallagher: An Overview and Some Projections, Japan-U.S. Seminar on Matrix Methods of Structural Analysis and Design, Tokyo, 1969, pp. 3-22.
33. D.R. Bland: The Associated Flow Rule of Plasticity, J. Mech. Phys. Solids, 6, 71-78.
34. P.S. Theocaris and E. Marketos: Elastic-plastic Analysis of Perforated thin strips of a strain-hardening Material, J. Mechanical Physical Solids, 12, 1964, p. 377-90.
35. O.C. Zienkiewicz: Elastoplastic Solutions of Engineering Problems-Initial Stress Finite Element Approach, Int. J. for Num. Method in Eng. 1, 1969, pp. 75-100.
36. D.N. Allen and R. V. Southwell, Phil. Trans. R. Soc. A242, 379, 1950.